PRODUCTION AND ANNEALING OF INTRINSIC DEFECTS IN X-RAY IRRADIATED CADMIUM SULFIDE

Technical Report No. 14

NASA NsG-573

GODDARD SPACE FLIGHT CENTER
Greenbelt, Maryland

by

K. W. Böer

Principal Investigator
Physics Department
University of Delaware
Newark, Delaware

PRODUCTION AND ANNEALING OF INTRINSIC DEFECTS IN X-RAY IRRADIATED CADMIUM SULFIDE

by

Joseph Charles O'Connell

A dissertation submitted to the Faculty of the University of Delaware in partial fulfillment of the requirements for the degree of Doctor of Philosophy in Physics.

June, 1967

ACKNOWLEDGEMENT

I wish to thank Dr. K. W. Böer for many hours of discussion and advice during the course of this work. I also thank Rudolph Schubert and Charles A. Kennedy for assistance in making measurements on numerous occasions. I am indebted to the Metallurgical Research Laboratory in Frankford Arsenal, Philadelphia for the use of their x-ray equipment and the technical assistance of Kurt Ritthaler and his co-workers. Finally I am grateful for the typing of the dissertation to my wife, Gayle.

This work was supported in part by the Research Group of the National Aeronautics and Space Administration.

ABSTRACT

"Pure" CdS single crystal platelets were exposed to x-rays of up to 300 keV at room temperature and liquid nitrogen temperature. Spectral distribution of photo current and thermally stimulated current measurements were made in ultra-high vacuum ($\sim 10^{-10}$ torr) before and after irradiation and after annealing above room temperature.

A model is proposed to explain the observed changes in these measurements based on displacement in the sulfur sublattice. An electron trapping level at $E_c - E_t = 0.5$ eV is identified as due to sulfur vacancies. In addition a recombination center is produced by sulfur vacancies diffusing to other defects to form associates. The damage produced anneals to a large extent after a heat treatment at 150°C. Further information is obtained from x-ray damage of crystals pre-heat treated in cadmium or sulfur vapor to shift the stoichiometry.

TABLE OF CONTENTS

CHAPTER I

Introduction

The diversity of the evergrowing number of semiconductor applications provide ample justification for the extensive activity in the field of intrinsic defects. Information of their effect on the electrical and optical properties of cadmium sulfide has been gained mainly by 1) shifting the stoichiometry by a heat treatment in the vapor of one of the components, 2) thermal damage, 3) radiation damage and 4) self-diffusion studies using radioactive tracers. The model proposed to account for the measured results by one investigator often disagrees with other models with the result that a single intrinsic defects is located at different energy levels in the band gap. This problem arises because of the complex nature of the defect structure of cadmium sulfide. Unlike impurities which can be introduced in large concentrations ($\sim 10^{18}$ cm^{-3}), compensation problems limit the concentrations of intrinsic defects. Usually the highest concentrations are of the same order of magnitude as the trace impurities in the "pure" crystals. In addition to this, defects may combine to form associates.

In the following work, x-rays (up to 300 keV maximum) were used as a source of radiation to alter the defect structure. The changes were detected by measuring the spectral distribution of photocurrent and thermally stimulated current curves. As a result of these

measurements, a model is proposed to account for the damage and its annealing.

CHAPTER II

Theory

2.1 Introduction. Since the electrical properties of any semiconductor depends greatly on the levels introduced into the band gap by imperfections, the identification of these levels in regard to what the microscopic disorder is that produces them and their characteristics (energetic position, charge state, capture cross-section, etc.) are quite important. The defect levels may arise from 1) impurities, 2) intrinsic defects, 3) surface, 4) dislocations etc.

Many impurities such as copper[1], indium[2,3], aluminum[2,3] etc. in CdS have been studied and their influence on the electrical properties are known. The concentration of these impurities is essentially fixed in a crystal during growth provided no further doping is carried out. The concentration at a particular site eg. in an unassociated interstitial position may change either by diffusion to a non-equivalent position (as in the case of Al in electron irradiated Si[4]) or by the proximity of another defect which leads to an associate.

Intrinsic defects on the other hand can be produced in a number of ways. First, there is a certain concentration introduced during growth which characteristically depends on the composition of the material transported to the surface, compensation requirements and the manner in which the crystals are cooled to room

temperature. This concentration may then be changed by intrinsic defects produced through Frenkel or Schottky disorder. Investigations of these mechanisms in CdS[5,6] show that intrinsic defects produced in this way have an activation energy of at least 2.5 eV and significant concentrations which are in thermal equilibrium, are important only at relatively high temperatures.

Two other methods of producing intrinsic defects are used in the following investigation, namely radiation damage and heat treatment in the vapor of one of the components.

2.2 Radiation Damage. The primary damage to a lattice in radiation damage is the displacement of an atom from its lattice site and results in a vacancy-interstitial pair. For heavy bombarding particles (α-particle, deuterons etc.) one produces not only random vacancy - interstitial pairs but disordered regions (subsequent displacements on neighboring sites caused by the primary knock-on atom). Since a complex defect structure already exists in cadmium sulfide, electron damage (or x-rays and γ-rays which produce energetic electrons by the photoelectric or Compton effect) is desirable.

The maximum energy that an electron of energy E_e may lose in a collision with a lattice atom is[7],

$$E_M = \frac{2(E_e + 2m_e c^2)}{Mc^2} E_e \qquad (1)$$

where M is the mass of the struck atom, m_e is the electron mass and c is the velocity of light. When the energy exceeds a certain energy E_d, the displacement energy, enough energy is transferred to displace an atom from its

lattice site. In CdS the displacement may be either a cadmium or sulfur atom, but because of the 1/M term in equation (1) approximately 3.5 times as much energy is transferred to the sulfur (32) than to the cadmium (112.4) at a particular energy E_e. Therefore the first energy threshold should be associated with damage in the sulfur sublattice.

In general, the displacement energies for semiconductors have not been extensively studied. A list of some of those reported is given in Table 1.

The value for S-displacement in CdS by Kulp and Kelley is based on the formation of two flourescence bands at 5140 Å and 7200 Å after 115 keV electron bombardment. Kulp showed that two more bands at 6050 Å and 1.03μ formed for irradiation with 290 keV electrons and associated this with cadmium displacement.

In addition to displacement caused by elastic collision, displacement in ionic crystals by mechanisms involving ionization have been proposed by Seitz[16], Varley[17], Williams[18], and others. Whether or not these mechanisms occur in CdS which has a pronounced ionic component is unknown although Garlick, Bryant and Cox[19] have proposed a Seitz mechanism to explain changes in the 1.63μ emission band in Co^{60} γ-irradiated CdS.

TABLE 1

Material	Displaced Atom	Threshold Energy(KeV)	Displacement Energy(eV)
Si[8]	Si	145	12.9
Ge[9]	Ge	360	15.1
InP[10]	In	274	6.7
	P	111	8.7
GaAs[10]	Ga	233	9.0
	As	256	9.4
InAs[10]	In	274	6.7
	As	231	8.3
InSb[11]	In	240	5.7
	Sb	285	6.6
CdS[12,13]	Cd	290	7.3
	S	115	8.7
ZnSe[14,15]	Zn	195	7.8
	Se	240	8.2

We then have $f>1$ and $|\theta_1| < |\theta_2|$ if $D> 4R$

and $f<1$ and $|\theta_1| > |\theta_2|$ if $D< 4R$.

For an equally spaced row of atoms, a sequence of collisions passes from atom to atom. The relation between θ_n and θ_{n+1} is

$$\theta_n = (-f)\ \theta_{n-1} = (-f)^2\theta_{n-2} = (-f)^3\theta_{n-3} = \ldots = (-f)^n\theta_o$$

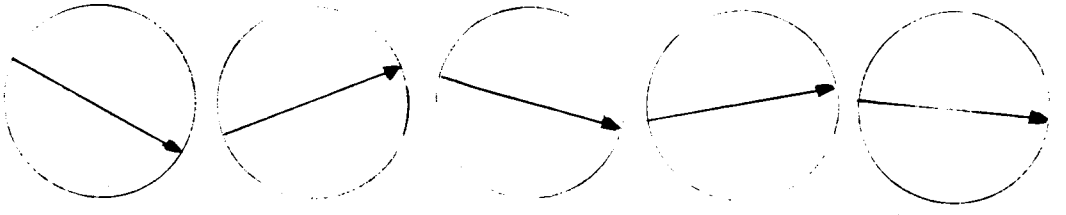

Figure 2

If $D > 4R$ and $f > 1$, θ_n diverges but for $D < 4R$ and $f < 1$, θ_n converges to zero with $(-f)^n$ and for equal masses, momentum transfer occurs with 100% efficiency. This type of transfer then favors close packed directions in the crystal.

Realistic calculations of this type of course require other than the hard sphere potential to take into account the "softness" of the atoms. For this case,

focusing replacements can occur where the struck atom replaces its neighbor leading to a vacancy at one end and an ejected atom at the other (eg. surface).

While evidence exists for focusing in metals from sputtering experiments[23], the effectiveness of this mechanism in a compound semiconductor is unknown. One can only say that the requirements for focused collisions would most easily be fulfilled in the sulfur sublattice because of the large size of the sulfur atom.

2.4 Defect Associates. The simplest type of damage that can occur is a random distribution of vacancies and interstitials throughout the crystal. However associates of these defects are known to be formed in Ge and Si, especially for irradiation at room temperature. The movement of vacancies has been reported[24] at temperatures as low as 120° K even though appreciable self-diffusion occurs only at much higher temperatures.

Van Gool and Diemer[25] have shown that associates of single point defects occur in the II-VI compounds and numerous levels obtained in thermally stimulated current data have been proposed to be due to associates. In addition, Colbow[26] has used a donor-acceptor pair model for the radiative recombination (edge emission) at 5175 Å at 4.2° K in CdS. Thus it is reasonable to suppose that associates will play an important role in the radiation effects in CdS.

Kroger[27] in "The Chemistry of Imperfect Crystals" has amply treated the subject of defect chemistry provided thermodynamic equilibrium exists in the defect structure or the non-equilibrium (frozen-in) state can be accurately specified. The defects produced by radiation damage are

obviously not in thermodynamic equilibrium. A brief digression to consider the formation and dissociation of associates in thermodynamic equilibrium however does give insight into the conditions favoring these two processes.

Let us imagine that there are two types of imperfections A and B randomly distributed throughout the crystal. There is a certain probability then that some A's and B's will be on adjacent lattice sites, i.e. associated. If, additionally, there are forces acting between the imperfections, the equilibrium concentration of associates will be greater (attractive forces) or less (repulsive forces).

We may represent the formation of an associate with an enthalpy increment ΔH by

$$A + B \rightleftarrows (AB) + \Delta H$$

If it is assumed that the single imperfections and associates are distributed ramdomly, the concentrations of these defects are linked by the mass action law

$$\frac{[AB]}{[A][B]} = K_{AB}$$

with

$$K_{AB} = \exp\ (-\Delta G/kT)$$

where ΔG is the variation in Gibbs free energy for the reaction at standard conditions,

$$\Delta G = \Delta H - T\Delta S.$$

The enthalpy effect may be due to Coulomb interaction, covalent bonding, etc. while the entropy variation is

associated with a configurational part and a vibrational part. Since the entropy contributions result in a pre-exponential factor in computing K_{AB}, they will be designated by C;

$$K_{AB} = \frac{[AB]}{[A][B]} = C \exp(-\Delta H/kT).$$

If only one type of associate is present e.g. A and B on nearest neighbor sites, then the conservation of mass law reads,

$$[AB] + [A] = [A]_{tot}$$

$$[AB] + [B] = [B]_{tot}$$

if we consider the relatively simple case where

$$[A]_{tot} = [B]_{tot}$$

the concentrations [AB], [A] and [B] can be found as a function of temperature for two specific ranges. At low values of $\Delta H/kT$ (small ΔH, low concentrations or high temperature) practically all imperfections are free and

$$[A] = [B] = [A]_{tot} = [B]_{tot}$$

so that

$$[AB] = [B]^2_{tot} \; C \exp(-\Delta H/kT),$$

$$\ln [AB] = 2 \ln [B]_{tot} + \ln C - \Delta H/kT.$$

At high values of $\Delta H/kT$ (large ΔH, low temperature or high concentrations) association is practically complete and

$$[AB] = [A]_{tot} = [B]_{tot},$$

$$[A]^2 = ([A]_{tot}/C) \exp(\Delta H/kT),$$

$$\ln [A] = 1/2 (\ln [A]_{tot} - \ln C + \Delta H/kT)$$

The dependence of association on temperature and concentration are given graphically below.

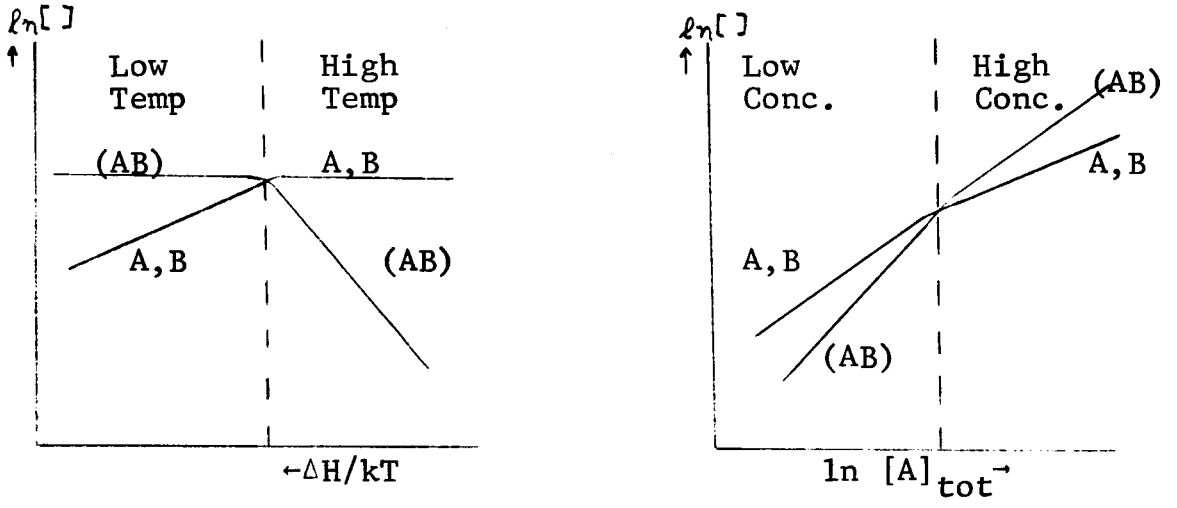

Figure 3

2.5 Levels in the Forbidden Gap. The products of radiation damage, whether associates or single point defects will give rise to levels in the band gap. These levels may be classified into three main categories namely, hole traps, electron traps and recombination centers. Traps are distinguished by the fact that the trapped electrons (holes) have a greater probability of

being thermally excited into the conduction (valence) band than to recombine with a free hole (electron). For recombination centers just the reverse is true.

The region of the band gap which contains electron traps can very simply be thought of as that lying between the conduction band edge (E_c) and the electron quasi-Fermi level ($E_{f,n}$) which is defined by

$$E_c - E_{f,n} = kT \ln(N_c/n) \qquad (2)$$

where N_c is the effective density of states in the conduction band and n is the density of free electrons. Actually the electron demarcation level should be used but for a first approximation this can be taken to be equivalent to the electron quasi-Fermi level. Similarly, hole traps are located between the hole quasi-Fermi level, defined in a manner similar to the electron quasi-Fermi level, and the valence band edge. The remaining area is occupied by recombination centers. This scheme is represented by the accompanying figure.

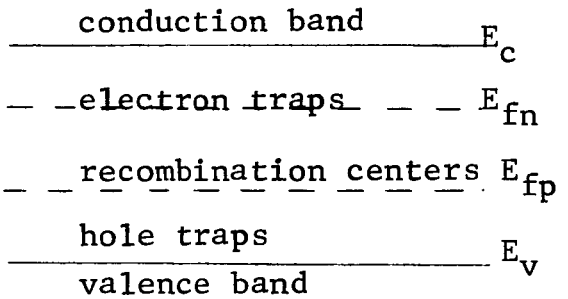

Figure 4

2.6 Spectral Distribution of Photoconductivity (SDP). By measuring the spectral distribution of photocurrent (which will be designated hereafter SDP) ie. photocurrent as a function of the wavelength of incident monochromatic light, one can gain information of levels in two of the three regions defined above. For photons of energy less than the band gap energy, excitation of electrons from levels below the quasi-Fermi level for holes occurs. Thus, an increase in the density of one of these levels could give rise to an increase in absorption by these centers resulting in a larger photocurrent at the photon energy corresponding to excitation from this level. This is best illustrated in CdS by using Cu as a dopant in varied concentration[28].

In addition since this is a kinetic process, at any particular wavelength an equilibrium between excitation and recombination must be reached. Therefore for the simple case where there is only one recombination level, an increase in the density of this level would decrease the electron lifetime and give rise to a lower stationary photocurrent. In this case a wavelength independent shift of the photocurrent in the extrinsic range would result. Of course the possibility of producing a parallel shift of this type can occur by other means, e. g. a decrease in a number of hole trap levels.

A major difference exists between absorption of photons of $h\upsilon > E_g$ and those of $h\upsilon < E_g$. The absorption coefficient goes from less than 1 cm^{-1} for extrinsic light ($h\upsilon < E_g$) to $>10^5$ cm^{-1} for intrinsic light ($h\upsilon > E_g$)[29]. The intrinsic light is totally absorbed in a very shallow region near the surface of the crystal. This effectively produces a higher excitation density of electrons in this

range. As can be seen from equation (2) an increase in the free electron density causes the electron quasi-Fermi level to move closer to the conduction band and converts electron traps to recombination centers. Additionally, surface recombination may be much larger than volume recombination[30]. This is due to the existence of more defects at the surface than in the bulk or defects having larger capture cross-sections. Adsorbed gasses in particular are known to influence both the dark and photoconductivity in CdS[31-33].

2.7 Thermally Stimulated Current Measurements (TSC). Thermally stimulated current curves gives information about the distribution of electron traps. This is effected by illuminating the crystal which causes electrons to fall into the electron traps and to prevent their thermal release by cooling the crystal to a low temperature. The illumination is then removed and the crystal is heated at a constant rate.

Let us examine just one discrete trapping level. As more thermal energy becomes available to the trapped electrons, their probability of escape to the conduction band increases. The freed carriers cause an increase in the TSC current. Recombination centers are continually removing carriers from the conduction band to reduce their non-equilibrium density. Eventually, the level is completely emptied. When the recombination rate is greater than the rate of thermal excitation from the trap, the TSC current decreases and therefore a current peak is associated with the trap. In real crystals, there is a distribution of trapping levels and one gains information about discrete levels only when their density is large enough to provide a well defined peak.

The simplest model for analyzing TSC curves which incorporates all of the basic features is given in the following figure.

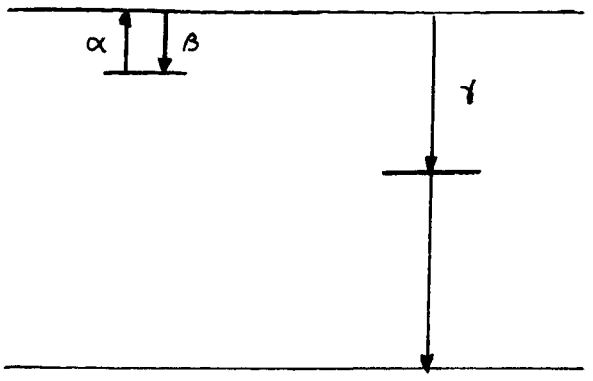

Figure 5

There is one trapping level a distance $E_c - E_t$ below the conduction band and having a capture cross-section for electrons S_t. The thermal emptying probability is

$$\alpha = \alpha^* \exp (E_c - E_t/kT) \qquad (3)$$

where α^* is the attempt to escape frequency. Electron capture is governed by

$$\beta = S_t v_{th} \qquad (4)$$

with v_{th} the thermal velocity of free electrons. Recombination occurs over a single level with a capture cross-section S_r and the recombination coefficient is

$$\gamma = S_r v_{th} \qquad (5)$$

The fate of an electron thermally released from a trap is then essentially determined by the relative magnitude of S_r and S_t. The two extreme cases are $S_r >> S_t$ and

$S_r \ll S_t$. In the first case, the released electrons simply proceed to recombination centers and a monomolecular process occurs. In the second case the electrons are retrapped many times before reaching a recombination center. This is usually referred to as the fast retrapping case.

The first theory along these lines was that of Randall and Wilkins[34] in which the energy $E_c - E_t$ is calculated from the temperature corresponding to a maximum in current for the case where $\beta = 0$ (no retrapping) by the expression

$$E_c - E_t = 25\ kT. \tag{6}$$

Many refinements have been made on this calculation and the two most commonly used are the heating rate method and the quasi-Fermi level method.

2.7.1 Heating Rate Method[35-37]. The temperature T_M corresponding to a TSC maximum is a function of the heating rate b. The energy $E_c - E_t$ is given by

$$E_c - E_t = kT_M \ln [N_c S_n v k T_M^2 / b(E_c - E_t)] \tag{7}$$

or

$$\ln(T_M^2/b) = (E_c - E_t)/kT_M - \ln[N_c S_n v k/(E_c - E_t)] \tag{8}$$

and by knowing the T_M for several heating rates, a plot of $\ln(T_M^2/b)$ versus $1/T_M$ gives $(E_c - E_t)/k$ as the slope.

2.7.2 Quasi-Fermi Level Method.[38] For fast retrapping, the trap can be considered to be in quasi-equilibrium with the conduction band and therefore the

position of the quasi-Fermi level coincides with the energy $E_c - E_t$ and

$$E_c - E_t = kT_M \ln(N_c/n_M) \qquad (9)$$

where n_M is the electron concentration of the current maximum.

2.7.3 Additional Information. In addition to the energy $E_c - E_t$, the density of traps and their capture cross-sections may be extracted. Our purpose is to detect relative changes in the density of existing levels or to detect new levels. Therefore the simple Randle Wilkins result suits our needs at this time. The temperature maxima and the heating rate are available for correlation with other work.

Finally, a trap may not only be characterised by an energy depth $E_c - E_t$ but may also have potential barrier of energy E_b associated with it. Due to the presence of potential barriers (repulsive traps) filling of these traps at low temperature is impeded[39]. Therefore TSC curves obtained by filling the traps at different temperatures yields information about the presence and magnitude of the barrier height E_b.

2.8 Sensitization. The stationary photocurrent, that is achieved when band gap light is considered in the model in Figure 5, can be increased (sensitized) by introducing other levels. The most common type of sensitization is due to the introduction of a second recombination center which has a capture cross section for holes of the same order of magnitude as the first center but has a much smaller capture cross section for electrons. Holes reaching these centers are effectively

stored and can not participate in recombination across the faster center. The sensitization of the crystal can be removed by freeing the stored holes either thermally or optically (quenching).

Clearly the concept of capture cross section is important here and levels which have small capture cross sections for carriers are repulsive traps, so that free carriers must have sufficient kinetic energy before they can become localized at the trap. While these levels might not normally be detected in electrical measurements, ionizing radiation such as x-rays, which can produce energetic carriers, could be capable of filling such levels. In this case, a high conductivity state exists until the carriers can be freed.

2.9 Previous Work. There has been a moderate amount of radiation damage work done on CdS. A number of investigations were prompted by the use of CdS crystals for detecting nuclear radiation[43]. These however are concerned with energy loss by ionization of electrons rather than by displacement.

Studies involving true damage to the lattice have been carried out using a wide variety of bombarding particles and detecting the defects through changes in electrical or optical properties as is seen in Table 2. While a model has been proposed to explain each of the individual measurements, a unified picture for the measurements en masse does not exist.

The major problems contributing to this situation are three in number; first, sample purity and preparation, second, the influence of the surface and irreversible changes and third, the production of complex defects by

irradiation at high energy and for massive particles.

Unlike germanium and silicon where impurities can be limited to 10^{13} cm^{-3}, "pure" CdS may be expected to have impurity concentrations $\sim 10^{16}$ cm^{-3} which is comparable to the concentration of intrinsic defects one expects to produce. In addition, the resistivity of "pure" crystals range in the literature from 1 ohm-cm to 10^{12} ohm-cm due to the degree of compensation. Thus for irradiation with comparable neutron flux, Galushka and Konozenko[44] saw a decrease in resistivity from 10^{11} - 10^{12} to 10^{8} ohm-cm and Oswald and Kikuchi[45] saw an increase from 2 ohm-cm to 10^{4} - 10^{6} ohm-cm.

Böer, Weber and Wojtowicz[46] and Böer and Gutjahr[47] have detected changes in the SDP with x-ray energies as low as 60 keV for measurements made in a vacuum of 10^{-6} torr. It is now felt that ionization of the gas ambient and subsequent bombardment of the crystal surface rather than interaction with the lattice atoms was responsible for the observed changes. Exposure to discharges of this type are known to effect the surface[48] and have often been used as a pre-treatment in an attempt to make ohmic contact to CdS crystals.[49,50]

A problem closely related to surface effects is the measurement of irreversible changes after irradiation. Galushka et al.[51] have measured the change in SDP in a vacuum of 10^{-4} torr for neutron and Co^{60} γ-irradiation. The extrinsic range decreases while the intrinsic range increases. No annealing is reported. Schweinberger and Wruck[52] also report large differences between extrinsic and intrinsic ranges in high vacuum (presumably $> 10^{-6}$torr) for 13.5 MeV deuteron irradiation.

Irreversible changes of this type are known to take place during the first vacuum heat treatment of a crystal. Studies using a mass spectrometer to detect gases desorbed from the surface during such a treatment, show a complex situation exists[53]. This is in contrast to the measurements here which are satisfying in that a damage-annealing cycle may be reproduced and the defects produced effect similar changes in the extrinsic and intrinsic ranges.

When energies in the MeV range are used for damage, displacement in both sublattices can take place. While the cross sections usually predict a greater production of defects in one or other of the sublattices, associate formation is quite probable since irradiations at liquid helium temperature have not been made. The deep trapping level at approximately $E_c - E_t = 0.6$ eV and numerous luminescence bands appear to be due to these associates.

Kulp and Kelley[12] have made a study of the threshold energy for displacement in CdS. For monoenergetic electrons above 115 keV, the edge emission (5140 Å) first increases and then decreases until it disappears. Accompanying this is the growth of a red luminescence band (7200 Å). These changes are irreversible, i.e. they don't anneal thermally. The edge emission is proposed to be due to sulfur interstitials and the red center to sulfur vacancies. The irreversibility is explained by radiation enhanced diffusion in which the electron beam sweeps the sulfur interstitials out of the crystal.

Edge emission has been studied for a number of years and several models have been proposed usually

involving the radiative recombination of a free carrier and a trapped carrier. The transition between these states, of course, is influenced by competing non-radiative transitions and these must be simultaneously studied before a change in luminescence can unambiguously be attributed to a change in the density of luminescing centers. Egorov et al.[63] have studied blue (exciton) and green (edge) luminescence excited by electrons whose energy is in the range 0 - 10 keV (cathodoluminescence). Unlike the blue luminescence which increases with increasing energy of the electron beam and becomes superlinear above 2.1 keV, the green luminescence saturates. The saturation occurs at different energies for different crystals and they conclude that this band is due to a center localized at the surface.

Kulp and Kelley's measurements were made in a vacuum of about 10^{-5} torr (pressure decreased somewhat when the crystal was cooled to low temperature) and it is noticed after prolonged electron bombardment that the surface of the crystal on which the electron beam is incident looks as if it has been etched[54]. This could account for the irreversible changes in the defect structure.

The excess sulfur produced at the surface during an irradiation is an interesting result since it is proposed for our results that this is the primary place for the production of damage. Rather than a radiation enhanced diffusion however, since no preferred direction exists for x-ray damage, the excess sulfur is most probably provided by focusing collisions. This requires only a transfer of momentum through the lattice and the actual displacement in the near-surface region. A clear

test of radiation enchanced diffusion by evaporating a radioactive isotope of sulfur on the crystal and measuring the diffusion profile after irradiation, in a manner similar to the work of Woodbury[55], has not been carried out.

Electron trap distributions have been measured by using either TSC measurements, the Niekisch method[56] (modulated light intensity) or Hall measurements. The most commonly reported levels produced by radiation damage are at 0.10 to 0.15 eV and 0.4 to 0.5 eV below the conduction band. In some cases correlation of different results is difficult because e.g. the temperature at the peak maximum and the heating rate are not given.

TABLE 2. PREVIOUS WORK

	Ref.	Type	Energy (MeV)	ρ	μ	P.C.	$E_c - E_t$ 0.05	$E_c - E_t$ 0.10 to 0.15 eV
Tanaka	57	deuteron	2	dec.		inc.		
Barjon	58	proton	1.4	dec.		inc.		
Broser	59	α	4.877	dec.		dec.		
Schweinberger	52	deutron	13.5	dec.		dec. (150°K) inc. (300°K)		inc.
Galushka	44	neutron	fast	dec.		inc.		inc.
Oswald	45	neutron	fast	inc.		inc.		
Galushka	51	neutron	fast	dec.	dec.	inc.		inc.
Galushka	51	γ-ray	1.2	inc.	dec.	dec.		inc.
Oswald	45	γ-ray	1.2	dec.				
Sera et al.	60	γ-ray	1.2	dec		dec		
Chester	61	γ-ray	1.2	dec.	dec.	inc.	inc.	inc.
Ibuki	62	γ-ray	0.67	dec.				
Garlick et al.	19	γ-ray	1.2	dec.				
Ibuki	62	electron	1.5, 1.8	dec.				
Kulp	12	electron	0.115	dec.				
Kulp	13	electron	0.29					
Lorenz et al.	64	electron	1.5	inc.				
Saito	65	electron	2.0					
Niekisch	66	electron	3.0					inc.
Collins	67	electron	3.0					

ρ = resistivity, μ = mobility, P.C. = photoconductivity

TABLE 2. PREVIOUS WORK (CONTD.)

	$E_c - E_t$			luminescence							
Ref.	0.42	0.48	0.59 to 0.65 eV	Blue	5140Å (edge)	6050Å	7200Å	8200Å	9600Å	1.05μ	1.63μ
57											
58											
59											
52	inc.		inc.								
44			inc.								
45				dec.	dec.		inc.				
51	inc.	inc.	inc.		dec.	inc.	dec.	inc.	inc.	inc.	
51	inc.				inc.		inc.				
45				dec.	dec.	dec.					
60											
61											
62											
19							inc.			inc.	inc.
62											
12					inc.		inc.				
13						inc.				inc.	
64											
65						inc.					
66		inc.									
67					inc.						

CHAPTER III

Experimental Arrangement

3.1 Equipment. The crystals used were grown in our laboratory by sublimation of CdS powder in a flowing atmosphere of H_2S and N_2. They were in the form of platelets with a surface area of up to 1 cm^2 and a thickness of 50-100μ. No intentional doping of these crystals was performed. The crystals selected had surfaces which were free from visible striations.

The crystals were then used in the "as grown" state or were heat-treated in cadmium or sulfur vapor. Heat-treatments were performed in quartz ampules which were first evacuated. The pressure on the pump side of the neck used for vacuum seal-off was 2×10^{-7} torr. The heat treatment temperatures and pressures are given in the following Table.

TABLE 3

	Temperature	Pressure
Cd vapor	700°C	10^{-2}torr
S vapor	800°C	10^{3} torr

Upon cessation of heat treatment, the quartz ampule could be dropped directly from the oven into a water bath for fast freezing-in of the existing defect structure.

An alternate Cd treatment was done utilizing a double oven (Fig. 6). A quartz tube consisting of two sections connected by a neck was evacuated by a mechanical pump. One section contained the crystals to be treated and the other a few grams of Cd. The temperature of the cadmium could be controlled by one oven to give a prescribed Cd vapor pressure and the temperature of the crystals was held higher than this by the other oven to prevent condensation.

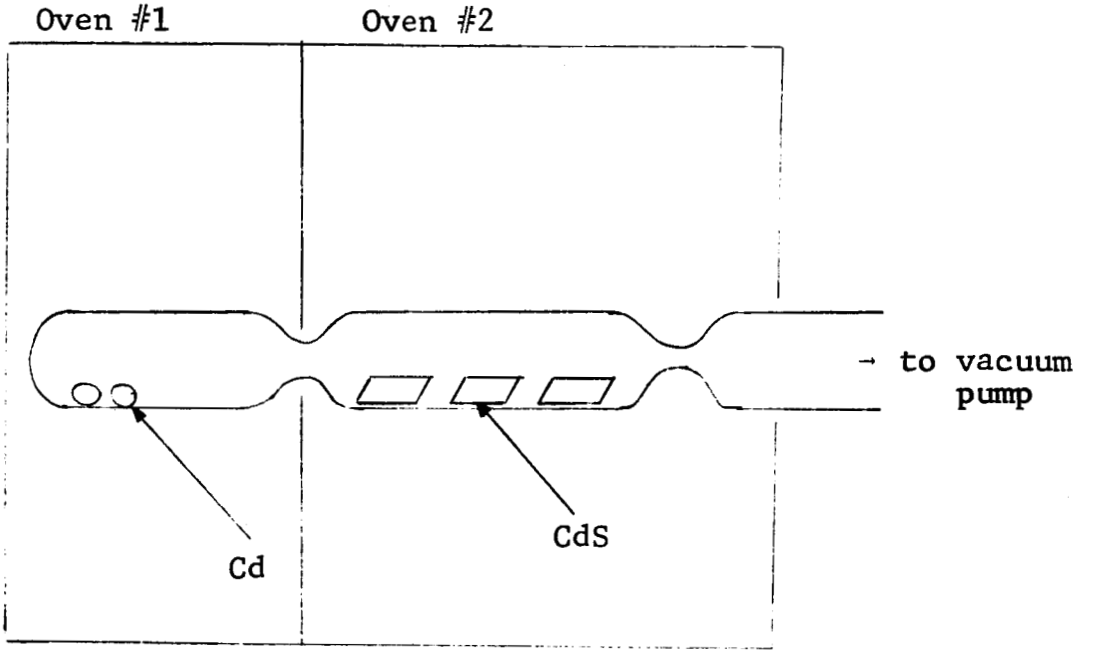

Figure 6

Heat treatments were carried out with the cadmium temperature T_{Cd} = 400°C giving a vapor pressure of approximately

1 torr. The temperature of the crystals was 500°C. Heat treatments at 600°C or higher caused considerable evaporation of the crystals. Temperatures were measured by chromel-alumel thermocouples in contact with the quartz below the Cd and CdS respectively. All heat treatments were carried out for a period of one hour.

Four gold-chromium contacts were then evaporated onto the crystals. The evaporation was performed in a vacuum of 10^{-7} torr. The gold was chosen for its stability at temperatures up to 350°C and the chromium was added to increase the mechanical stability by pinning dislocations.

Two crystals were then placed on a mica sheet which rested on a copper block (Fig. 7). The two crystals mounted were always of the same type to prevent any cross contamination, i.e. two untreated, two sulfur treated or two cadmium treated crystals. Gold wires were then held in place on the contacts by the tension in mica strips attached to the copper block. The tension also served to hold the crystal in place. Gold leaf was interposed between the gold wire and the evaporated contacts to minimize scratching. Thin coppper wires were then connected to the gold wires for electrical measurements.

A copper-constantan thermocouple was placed on a mica sheet of the same thickness as that separating the crystals from the copper block. Measurements with two thermocouples on a similar system[40] showed a temperature gradient of less than 1°C over the length of the copper block in the temperature range investigated.

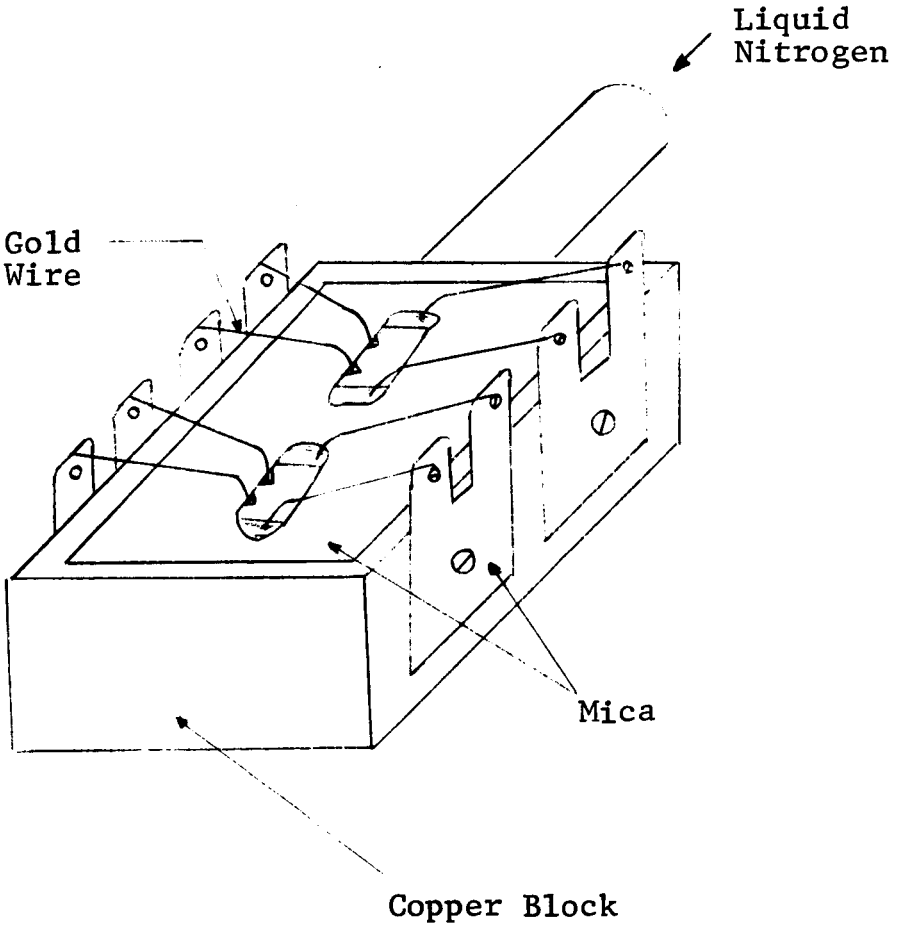

Figure 7. Crystal Holder

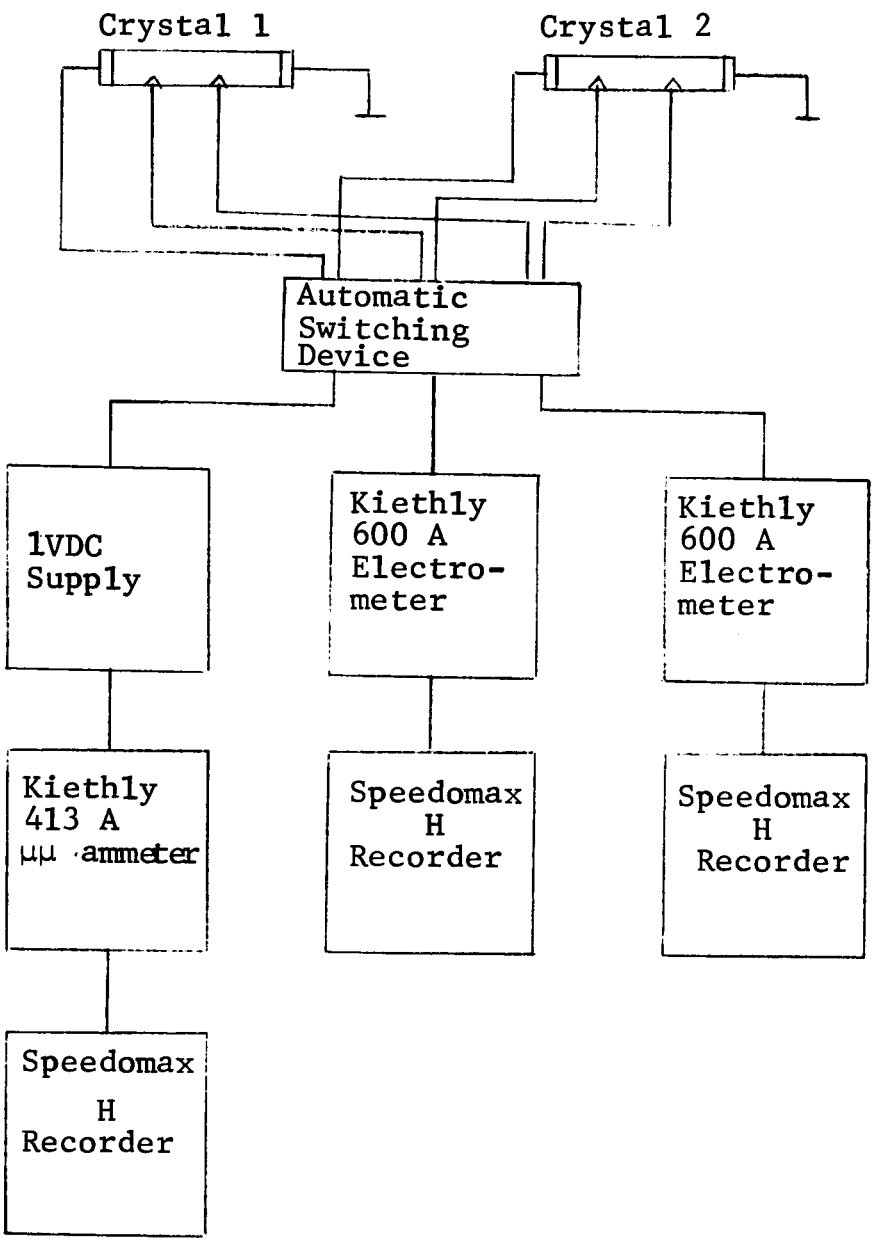

Figure 8. Electrical Measurements System

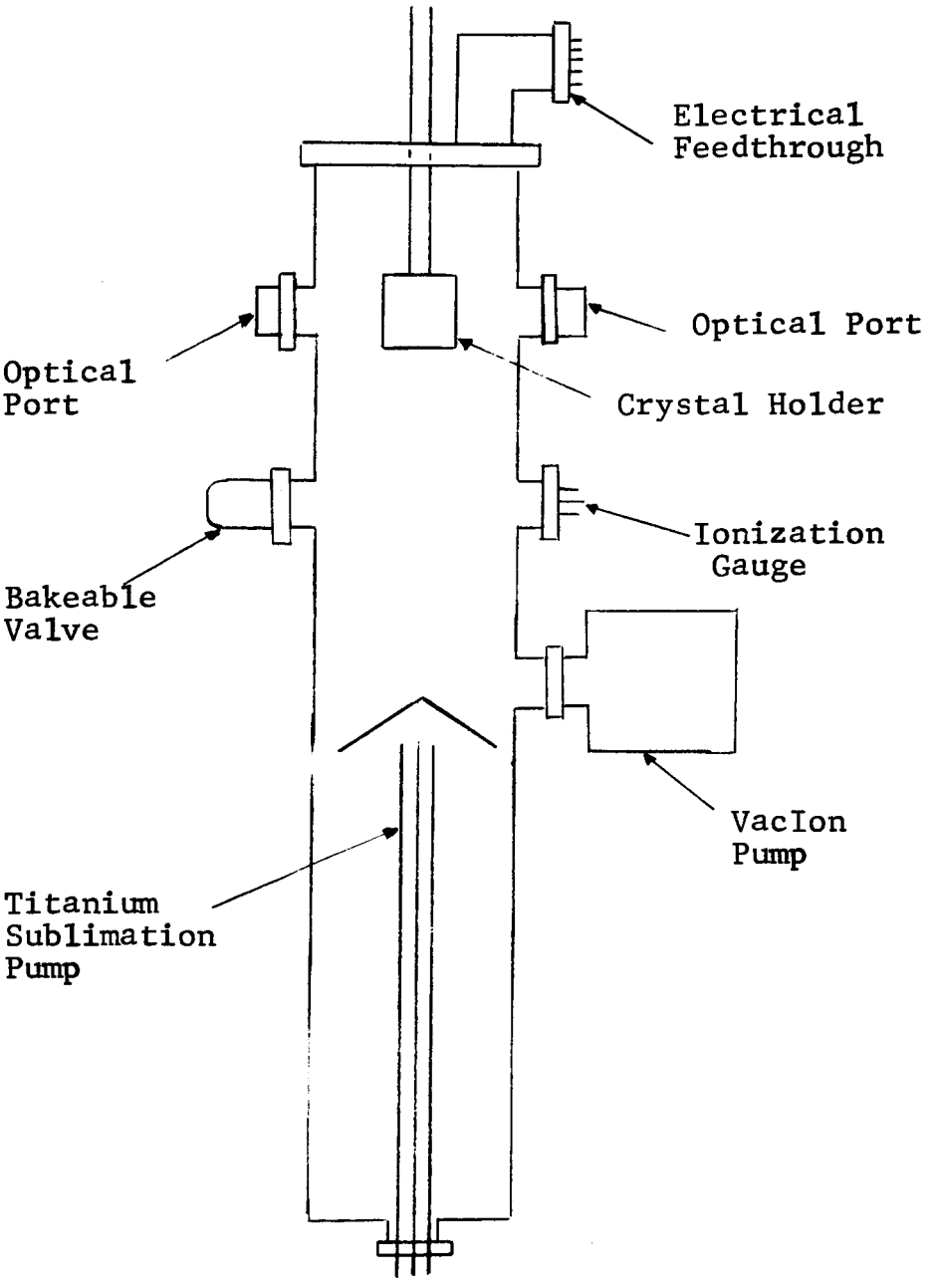

Figure 9. Vacuum System

The two large outer electrodes were connected in series with a Kiethley 413A logarithmic micro-micro-ammeter and a 1 V DC source (Fig. 8). The smaller inner electrodes were used as potential probes and were connected to two Kiethley 600A electrometers. The use of these probes was necessitated because of the nonohmic contacts. The experimental data given later are in units of conductance i.e. current divided by the potential difference at the probes and hence do not include barrier layer effects. The readings of the ammeter and electrometers were displayed on Leeds and Northrup Speedomax H recorders.

The copper crystal holder which was situated on the end of a stainless steel cold finger was mounted in an ultra-high vacuum system (operation in the 10^{-11} torr range) constructed to specifications by Varian Associates (Fig. 9). It consisted of a stainless steel cylinder with the following connections made by Varian Con-Flat flanges: 1) octal feedthrough for electrical and temperature measurement, 2) two glass viewing ports, 3) a bakeable ultra-high vacuum valve, 4) a nude ionization guage for measuring pressure down to 4×10^{-11} torr, 5) a 15 1/s Super VacIon pump, 6) a titanium sublimation cartridge and 7) a VacSorb pump which was used for roughing the system and could subsequently be disconnected by utilizing the bakeable valve.

Monochromatic light was obtained from a high intensity Bausch and Lomb monochromator, Model #33-86-40 with tungsten light source #33-86-37-01. The spectral half-width for the slit settings used is 5 mμ. Its output as a function of wavelength and the number of photons actually incident on the crystals as a function of wavelength are given in Fig. 10. The monochromator was

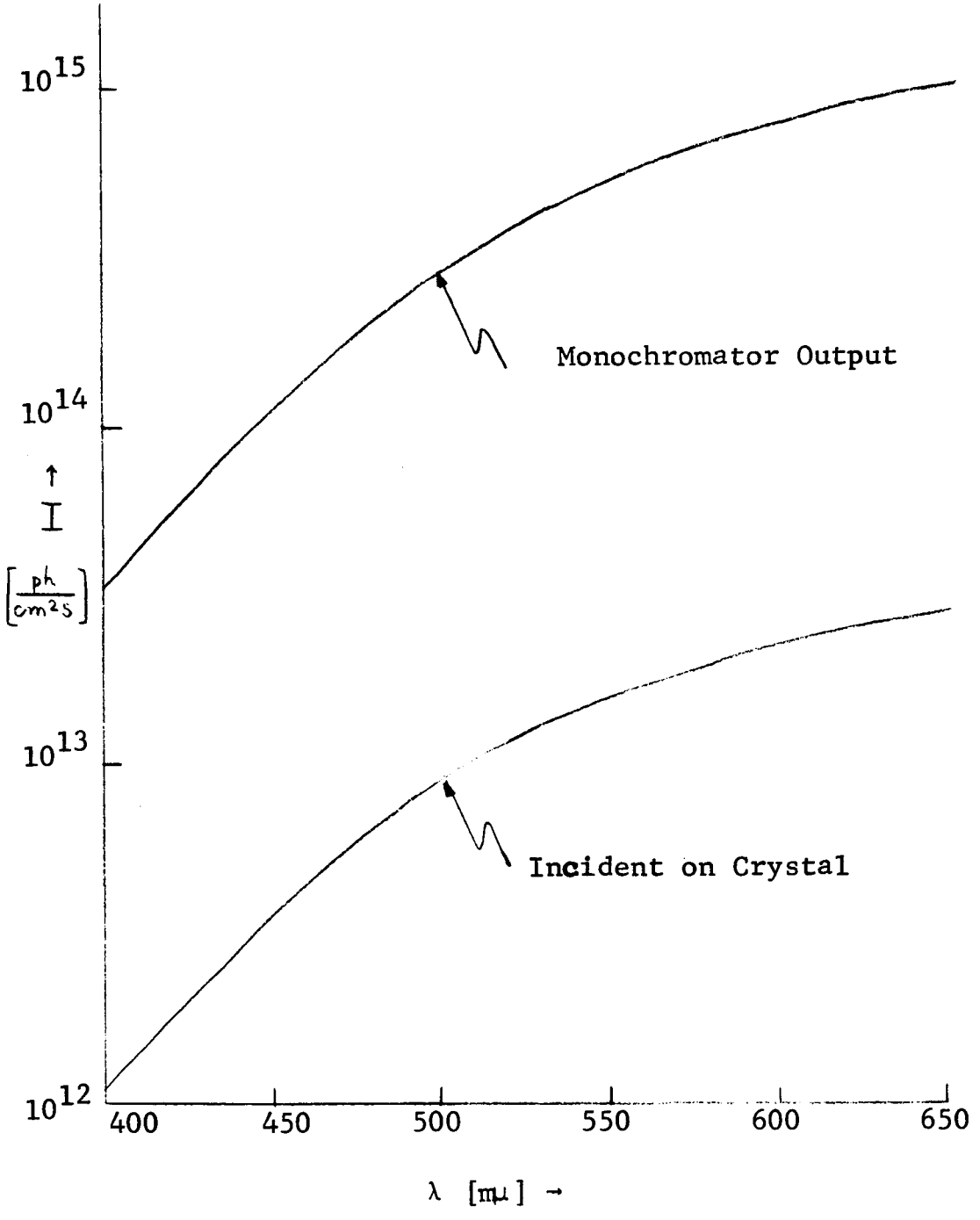

Figure 10. Number of photons from monochromator and incident on crystal as a function of the wavelength of light.

driven by a motor at a rate of 20 mμ/hr. This rate was sufficient to insure an equilibrium value of the photocurrent during spectral distribution of photocurrent measurements.

A solenoid exhaust valve was operated in a open-shut cycle by an electric timer used to pump liquid nitrogen from a sealed dewer if the SDP was to be measured at -190°C.

The x-ray source used was located in the Metallurgy Research Laboratory in Frankford Arsenal, Philadelphia. The tube had a tungsten anti-cathode and provided a maximum accelerating voltage of 300 kV and a maximum tube current of 15 ma. The spectrum of x-rays from such a source is made up of a continuous distribution from a maximum energy to lower energies (Bremstrahlung) and sharp lines characteristic of the target material. For tungsten, the highest energy line is 50 keV, much lower than the energy needed to produce damage. The continuous distribution can be represented by the equation[41]

$$I_\lambda = CZ \frac{1}{\lambda^2} \left(\frac{1}{\lambda_o} - \frac{1}{\lambda}\right) \qquad (10)$$

where C is a constant, Z is the atomic number of the target material and λ_o is the wavelength of the most energetic photon produced (Duane - Hunt limit).

An estimate of the flux of x-rays incident on the crystals has been made by integrating the number of photons in the energy range 250 to 300 keV. This yields a flux of 5×10^{12} photons/cm^2 for an exposure time of one hour. The crystals were placed at a distance of 45 cm from the anti-cathode. If the irradiation was

to be done at low temperature, liquid nitrogen was continuously pumped into the cold finger. Immediately upon cessation of room temperature irradiations, the crystals were cooled to -190°C. All crystals remained at this temperature for about 1 1/2 hrs. during the trip back to the laboratory.

3.2 Procedure. Care was taken during the starting of the VacIon pump to initiate pumping action as rapidly as possible in order to minimize the effect of ion bombardment on the surface of the crystal. This is accomplished by roughing below 10μ with the VacSorb pump and then firing the Ti-sublimation pump in a one minute on - five minute off cycle for several cycles. After this procedure, the pressure fell below 10^{-6} torr within 10 seconds after starting the VacIon pump.

The entire vacuum system was then baked-out for several hours at 300°C. The crystals however were maintained below 180°C to minimize changes in stoichiometry by evaporation of one component from the crystal. This is especially important for those crystals heat-treated in Cd or S-vapor. Upon cooling to room temperature the pressure fell below the guage limit of 4×10^{-11} torr. After several months the pressure was in the measureable 10^{-11} torr range.

A series of spectral distribution of photocurrent curves were then obtained to insure reproducible measurements. Likewise, a number of TSC measurements were made to detect any differences in trap distributions, namely, filling with 490 mμ and 650 mμ to detect differences between the bulk and surface-near region and filling at room temperature and liquid nitrogen temperature to

detect traps having energy barriers associated with them.

Once reproducible measurements were obtained for the untreated crystals, the SDP and TSC curves were measured after room temperature irradiations of 150, 250 and 300 keV x-rays. Since, as will be seen in the next chapter, only the 300 KeV irradiation produced significant changes in the two measurements, the majority of the following irradiations were at this energy.

Irradiation of untreated crystals were carried out at both room temperature and at liquid nitrogen temperature. After the irradiation, a spectral distribution was measured at liquid nitrogen temperature and then a TSC curve (490 mμ excitation) was run up to room temperature. The crystals were then stored in the dark at room temperature for several days and the measurements repeated.

The crystals were then heated to 100°C for one hour, cooled to room temperature and allowed to stabilize. A SDP and TSC curve were measured. The annealing was increased in 50° steps up to 300°C. For annealing at 150°C and higher, the cooling to room temperature was along the path in Fig. 11. This sequence of measurements hereafter will be referred to as a damage-annealing cycle. Many cycles of this type were run on a crystal (up to eight for one crystal) before it was removed from the vacuum system.

Crystals heat treated in cadmium of sulfur vapor were irradiated at 300 keV followed by a TSC curve (490 mμ) to room temperature and then a SDP curve. The remaining part of the damage-annealing cycle was identical to that for the untreated crystals.

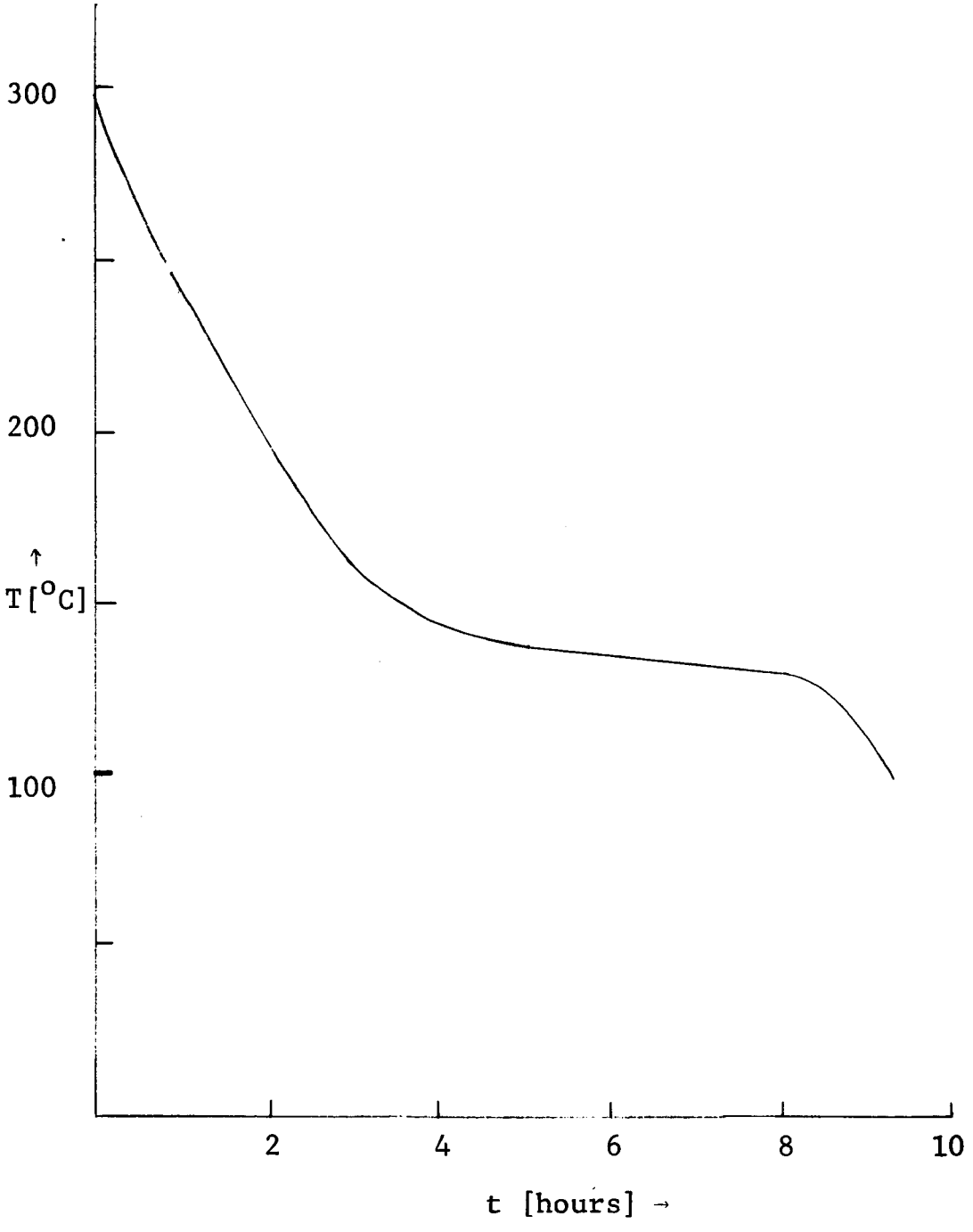

Figure 11. Annealing Curve

CHAPTER IV

Experimental Results

4.1 Untreated Crystals. The first quantity of interest was the lowest threshold energy for the production of electrically active defects. Irradiations at 150 and 250 keV carried out in ultra-high vacuum showed less than 10% change in the SDP which falls within the error of the measurement (Fig. 12). However, irradiation at 300 KeV at room temperature produced changes of almost an order of magnitude (Fig. 13, Curves 1,2,3). The SDP exhibits an almost parallel shift toward lower photocurrent and this shift proceeds further if the crystal is stored at room temperature. The TSC curves corresponding to this same cycle (Fig. 14, Curves 1,2,3) show a decrease in the peak at 180°K and an increase in the 300°K peak, followed by a decrease in both peaks. The defects producing these changes are stable at room temperature for several weeks after which time some partial annealing is evident (Fig. 15). Annealing can be accomplished by a 150°C heat treatment for one hour and cooling to room temperature along the curve in Fig. 11.

The damage-annealing cycle given above was repeated a number of times and a rather good reproducibility was obtained. The limiting factor on the number of irradiations a crystal could be subjected to was the quality of the contacts. Eventually the voltage difference at the potential probes became prohibitively small indicating

the presence of barrier layers at the current carrying contacts and the crystals were removed.

Damage-annealing cycles for x-ray damage at liquid nitrogen temperature were performed on the same crystals. These irradtions were carried out between room temperature damage-annealing cycles so that for one crystal up to eight cycles were made. For irradiation at low temperature, little change is seen in the SDP after damage (Fig. 15) but a similar behavior to irradiation at room temperature occurs upon storing the crystal at room temperature i.e. wavelength independent shift to lower photocurrents. The TSC peak at 180°K shows no change while the 300°K peak increases (Fig. 17). Again annealing occurs at 150°C.

For a crystal which was subjected to many damage-annealing cycles, a saturation effect was observed for room temperature damage, i.e. if the relative change in photocurrent at a particular wavelength (e.g. 600 mμ) before and after irradiation is taken as a measure of the damage, the curve in Fig. 18 results. For x-ray damage at room temperature, the sensitivity to damage decreases with the number of cycles, while for x-ray damage at liquid nitrogen temperature where the relative changes are small, no change in sensitivity is seen.

4.2 Sulfur Pre-treated Crystals. Since the contacts on the untreated crystals were attacked by the sulfur vapor during a heat treatment[68], crystals similar to the untreated crystals were used which had been pre-treated before the contacts were applied. These crystals when subjected to a damage cycle showed essentially no change in SDP (Fig. 19, Curve 1,2). The photocurrent

at liquid nitrogen temperature for the intensity used was below the detection limit of our ammeter (10^{-12} amp) and no useful information was derived from TSC measurements. These crystals did show a broad TSC peak at 440°K as previously reported by Kennedy[40]. This peak is proposed to be due to the aggregation of cadmium vacancies.

Normal behavior, i.e. damage-annealing cycles characteristic of the untreated crystals could be obtained after a heat treatment in vacuo at 350°C (Fig. 19, Curves 1', 2') although the magnitude of the shift in the SDP was considerably reduced.

4.3 Cadmium Pre-treated Crystals. Crystals heat treated in cadmium vapor in a closed tube in general had a prohibitively high dark conductivity ($\sim 10^{-2}\Omega^{-1}cm^{-1}$) and essentially no photosensitivity. A few crystals heat treated in the same ampule had dark conductivities as low as $10^{-9}\Omega^{-1}cm^{-1}$ and were photosensitive. These crystals were exposed to 300 keV x-rays and during the first damage-annealing cycle (SDP Fig. 20 and TSC Fig. 21) showed the following similarities to damage-annealing cycles of untreated crystals; first, a decrease in photocurrent which decreases even further upon storing the crystal at room temperature, second, an increase in the TSC curve at 300°K after irradiation and third, annealing occurs at about 150°C. The differences between this cycle and a cycle for untreated crystals are evident in the absence of parallel shifts of the SDP curves. In addition the growth of the TSC curve at 300°K appears to be due to an increase of a higher temperature peak i.e. only the low temperature tail is measured.

Subsequent damage-annealing cycles failed to show reproducible results and after the fourth irradiation, the crystal showed persistent photoconductivity, i.e. upon exposure to extrinsic light at liquid nitrogen temperature the photocurrent rises to a steady state value and remains there even after the excitation is removed. This state can be destroyed by heating the crystal to room temperature.

Crystals pre-treated in cadmium vapor in an open tube* behaved in the following manner upon irradiation. After irradiation at room temperature and cooling the crystal to liquid nitrogen temperature, the current through the crystal was increased by up to three orders of magnitude (Fig. 22). In addition, the potential difference between the two potential probes and between the probes and the anode was very small compared to the one volt drop between the cathode and the anode. This indicates a high resistance region near the cathode. Exposure to light of wavelength λ=490 mμ causes first an increase in crystal current and then the onset of two processes indicated by the two step decrease in crystal current until a value of the photocurrent equivalent to the pre-irradiated one is reached. During this time, the potential distribution also reaches its pre-irradiated value.

---

* This type of treatment was used to provide a constant supply of cadmium vapor to the atmosphere surrounding the crystal. In investigating the effect of adsorbed oxygen on the electrical properties of CdS crystals[69], a flowing oxygen atmosphere gives markedly different results than backfilling in a closed system. In a closed system, the partial pressure of oxygen decreases because the oxygen replaces gases already adsorbed on the container surfaces.

The SDP and TSC curves are given in Fig. 23 and 24. They show essentially no change before and after irradiation. A vacuum heat treatment of this crystal at 350°C produced a decrease in dark conductivity and an increase of photosensitivity but no changes in the damage-annealing cycle.

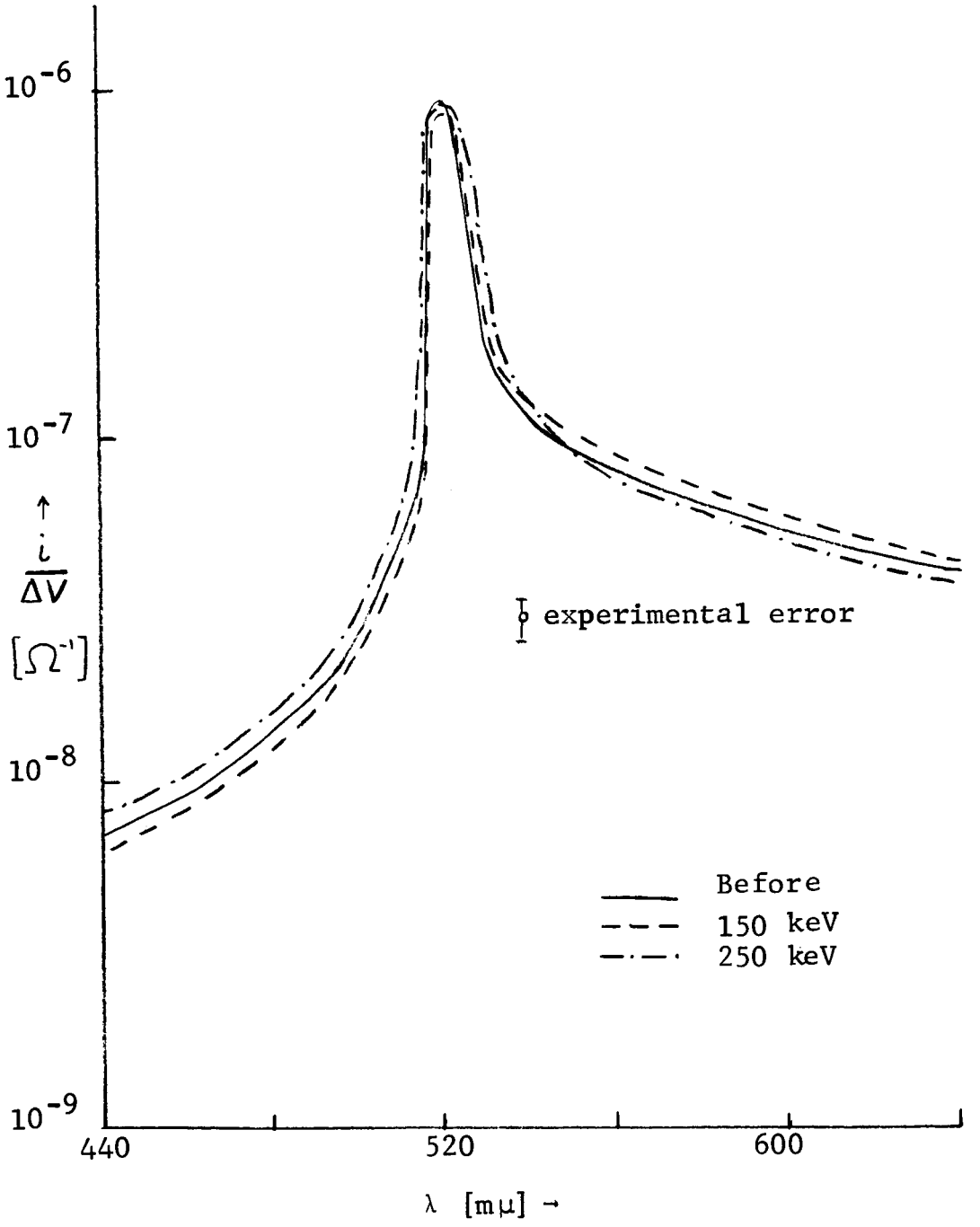

Figure 12. SDP before and after x-ray irradiation at 150 and 250 keV. Irradiation at room temperature, SDP measured at 25°C. The indicated error is the same for subsequent measurements.

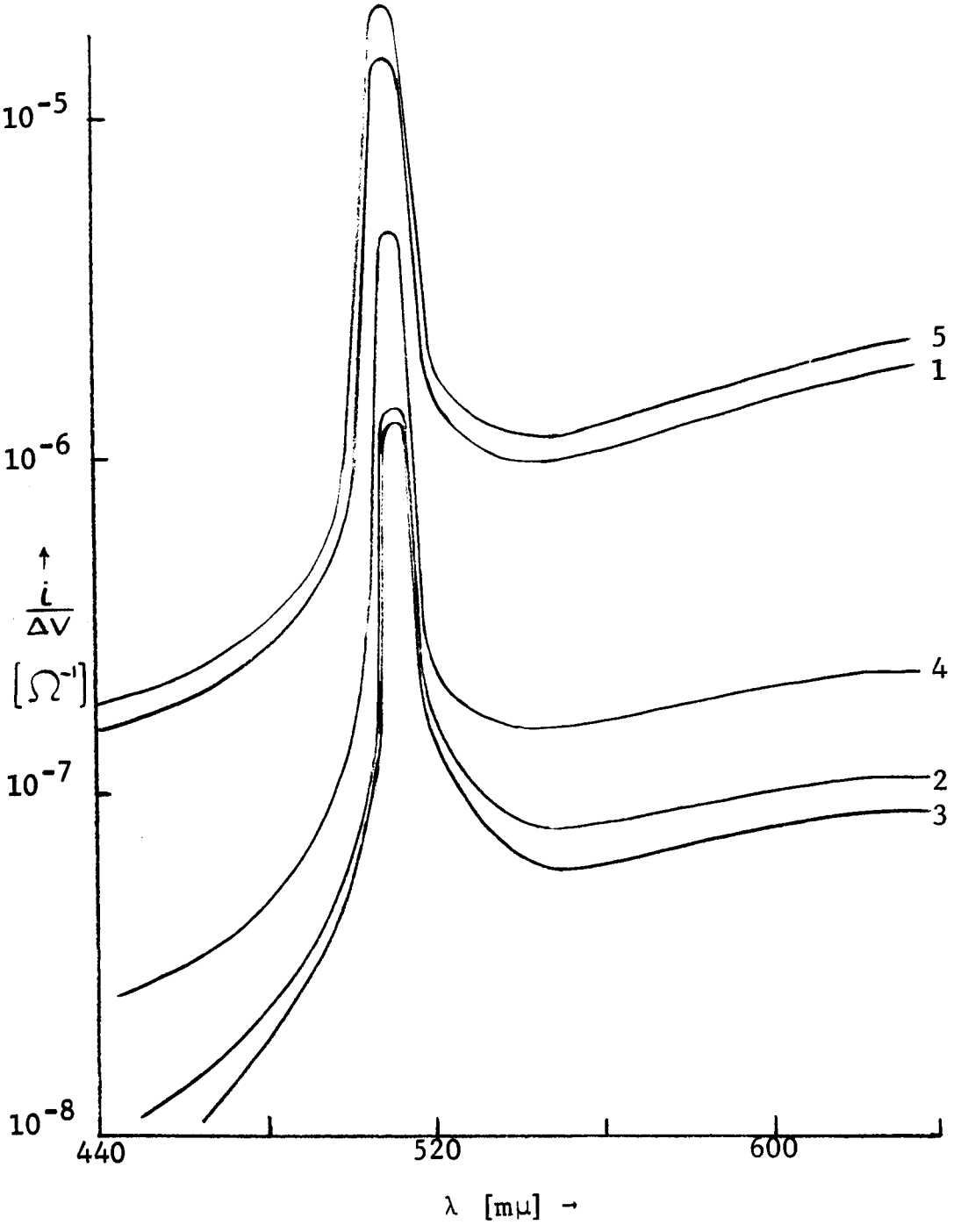

Figure 13. SDP 1) before and 2) after 300 keV x-ray irradiation at room temperature 3) 6 day later and after annealing at 4) 100°C and 5) 150°C. SDP measured at -190°C.

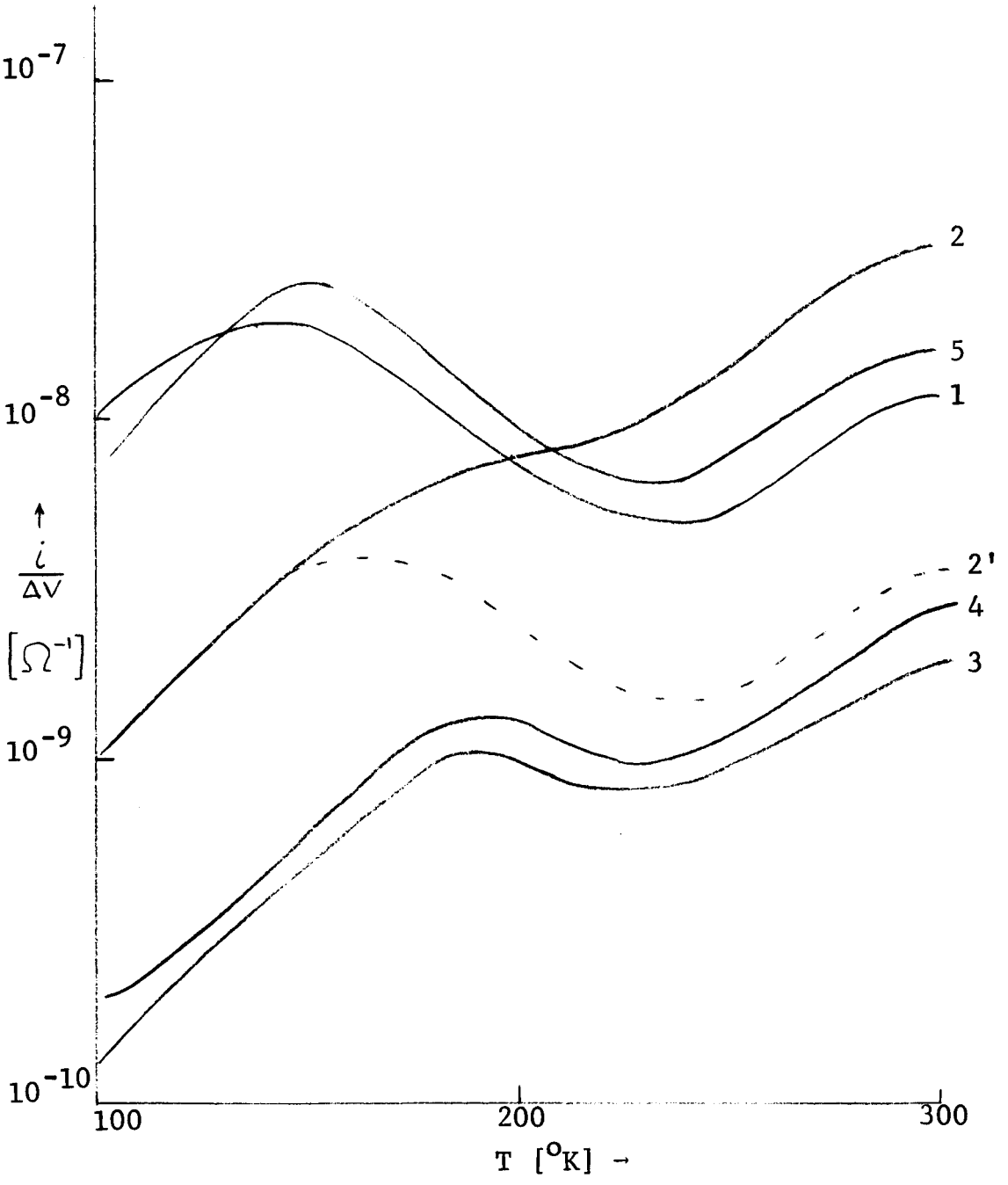

Figure 14. TSC curves 1) before and 2) after 300 keV x-ray irradiation at room temperature; 3) 6 days later and after annealing at 4) 100°C and 5) 150°C. (490 mμ excitation). Curve 2' is an expected result not a measurement.

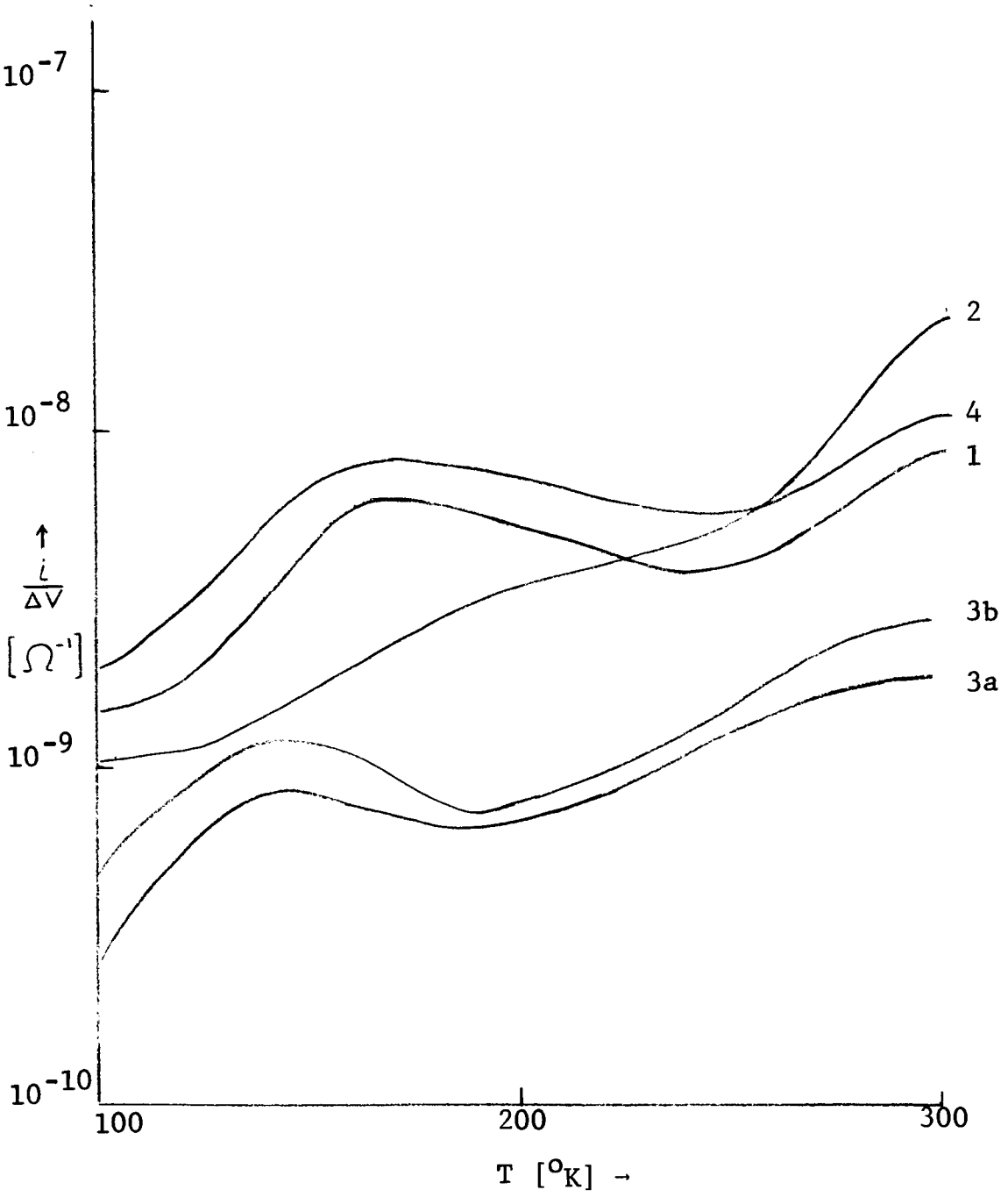

Figure 15. TSC curve 1) before and 2) after 300 keV irradiation at room temperature 3a) after 6 days; 3b) after 16 days at room temperature and 4) after annealing at 100°C (490 mμ excitation).

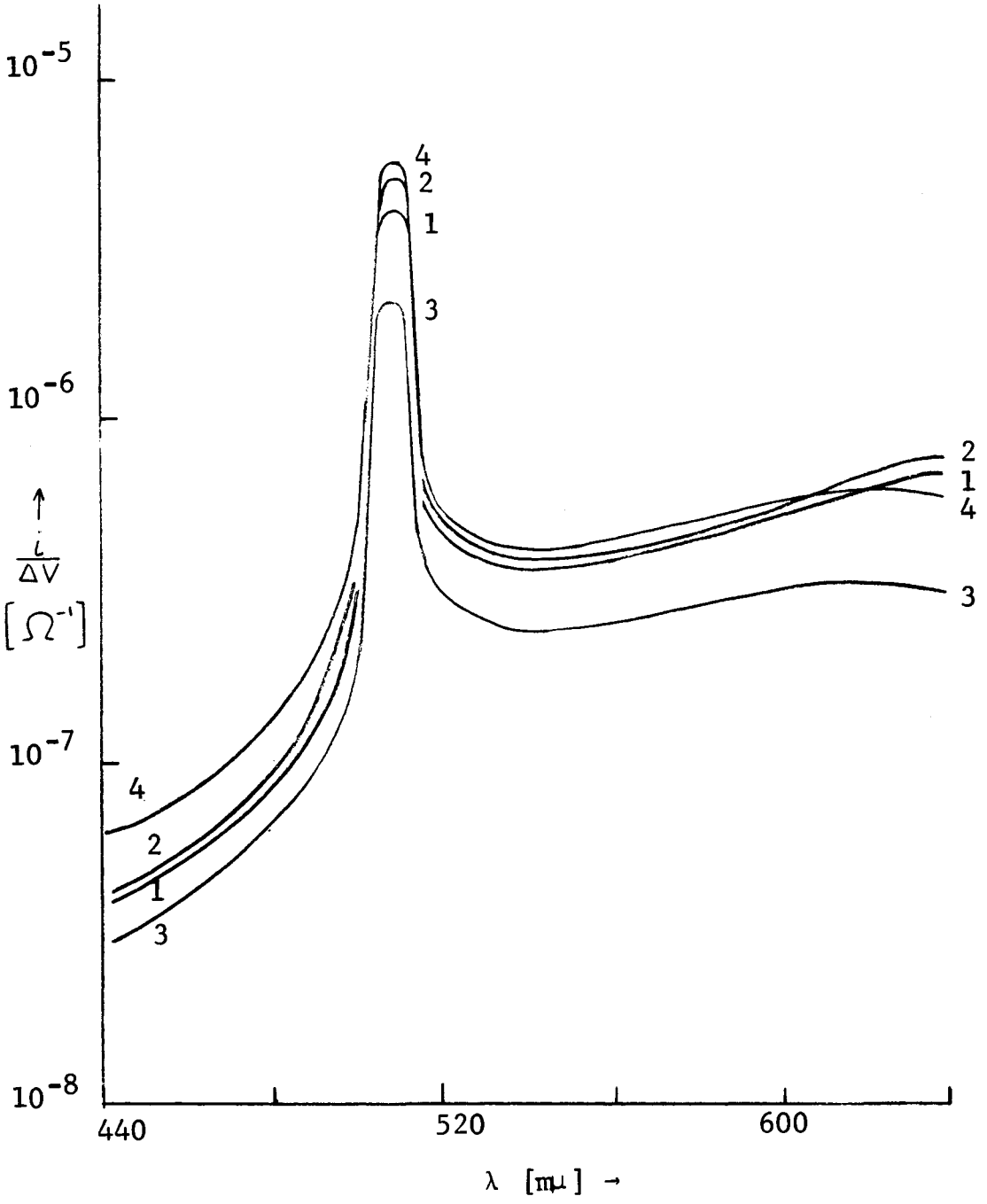

Figure 16. SDP 1) before and 2) after 300 keV x-ray irradiation at liquid nitrogen temperature 3) after 6 days and 4) after annealing at 100°C. SDP measured at -190°C.

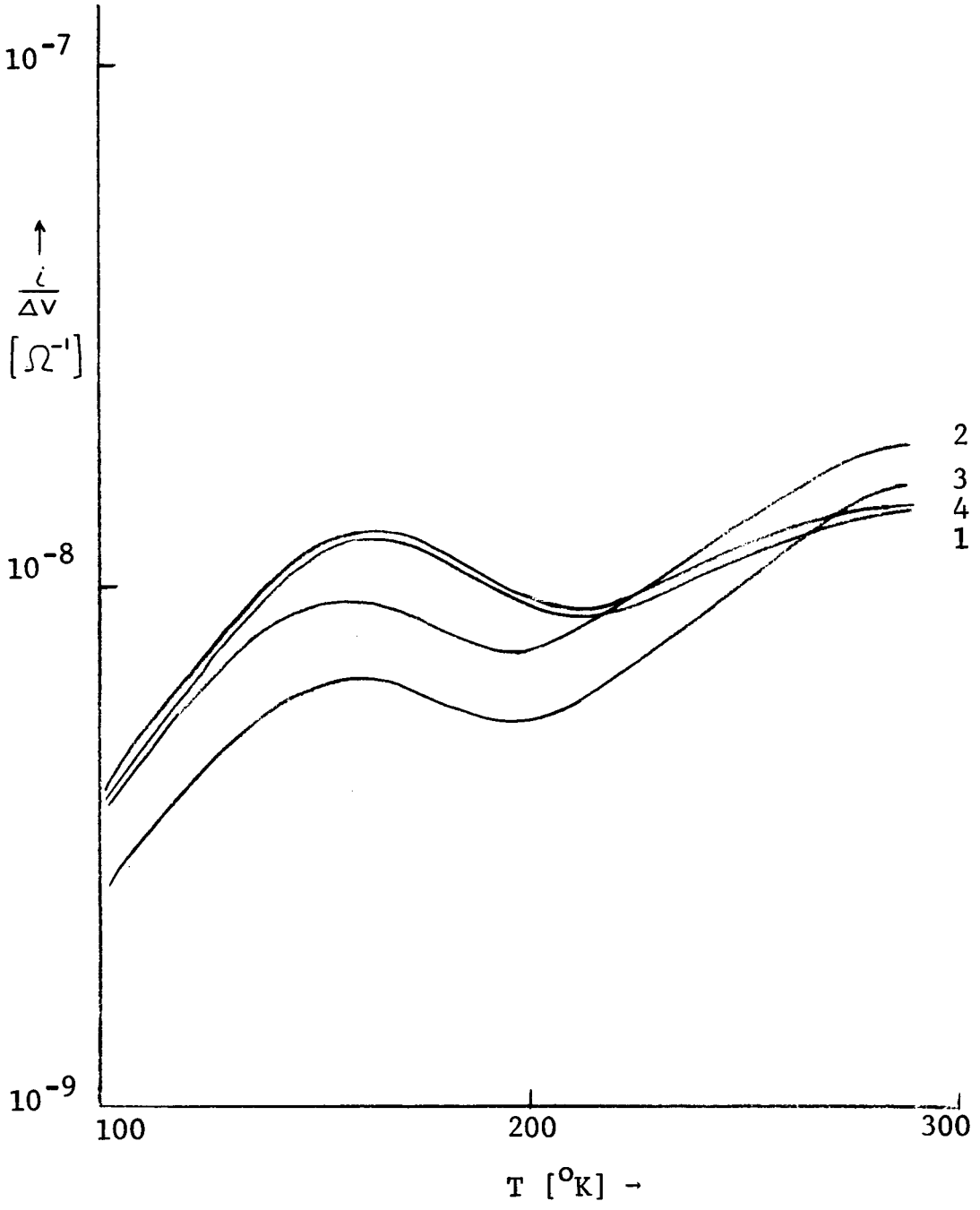

Figure 17. TSC curves 1) before and 2) after 300 keV x-ray irradiation at liquid nitrogen temperature, 3) after 6 days and 4) after annealing at 100°C (490 mμ excitation).

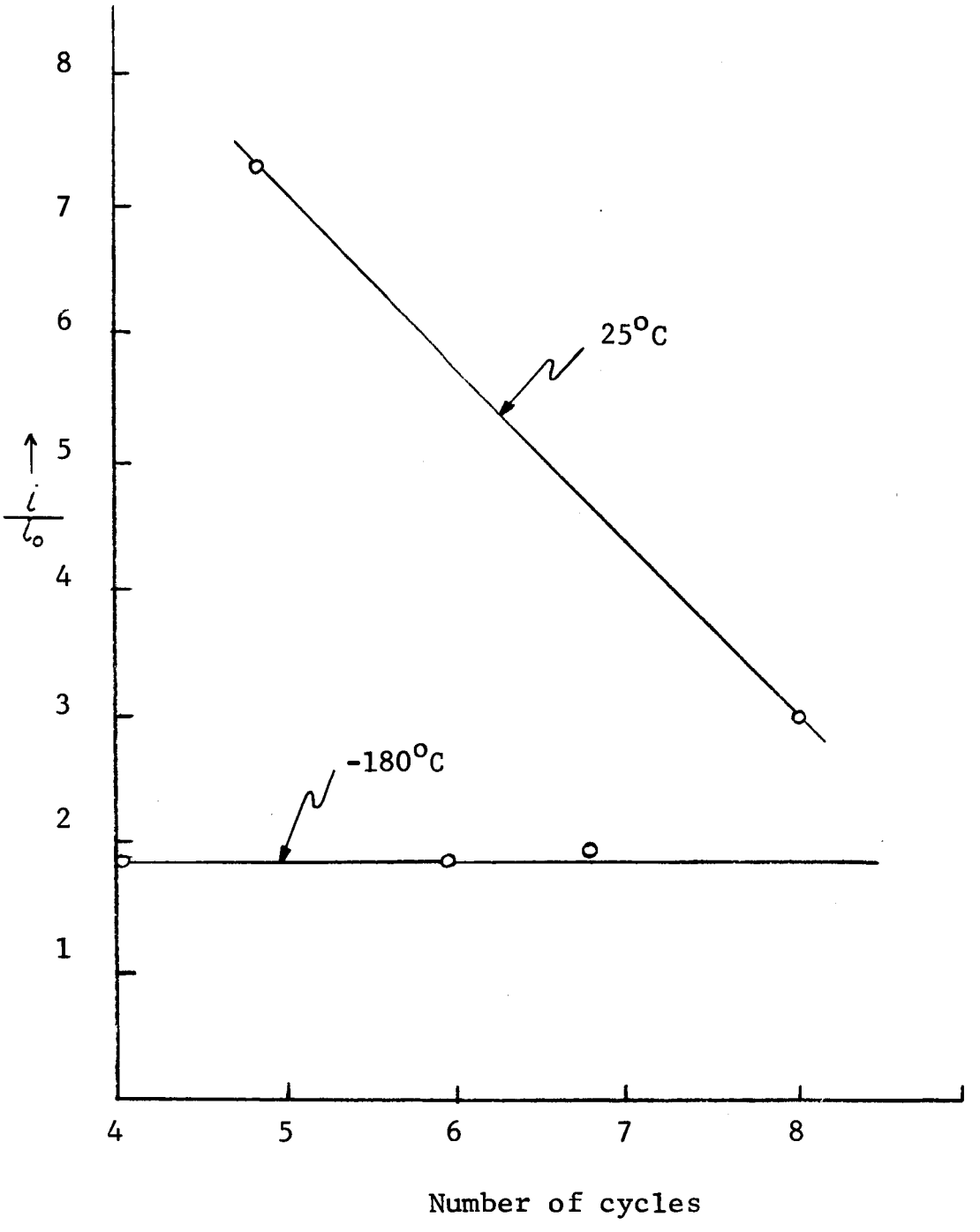

Figure 18. Relative change in photo current at 600 mμ before and 6 days after 300 keV x-ray irradiation at 25°C and -190°C.

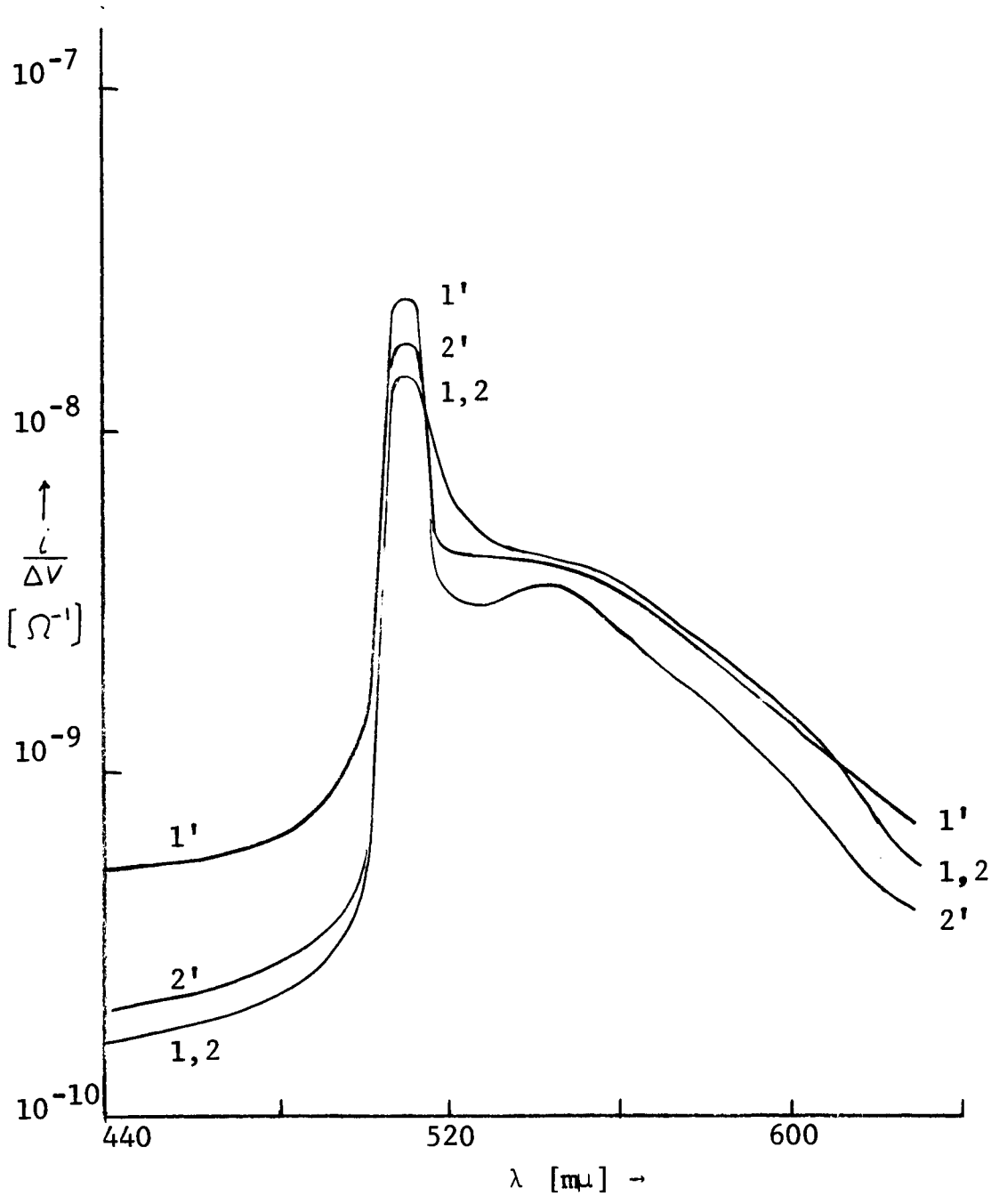

Figure 19. SDP for sulfur (1,2) and vacuum (1', 2') heat treated crystal before and after 300 keV x-ray irradiation at room temperature SDP measured at 25°C.

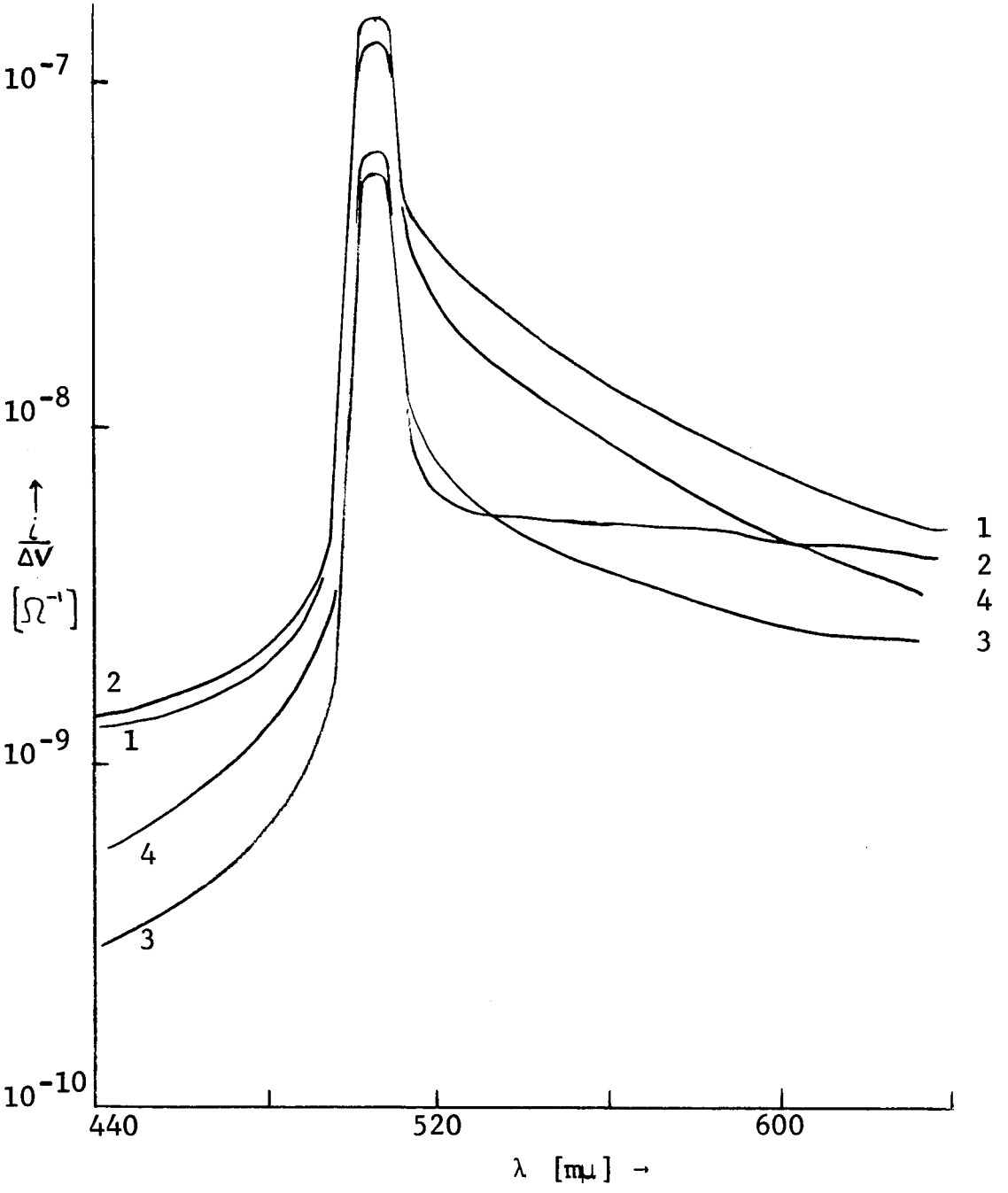

Figure 20. SDP for cadmium treated (closed tube) crystal 1) before and 2) after 300 keV x-ray irradiation at room temperature, 3) after 6 days after and 4) after annealing at 100°C. SDP measured at 25°C.

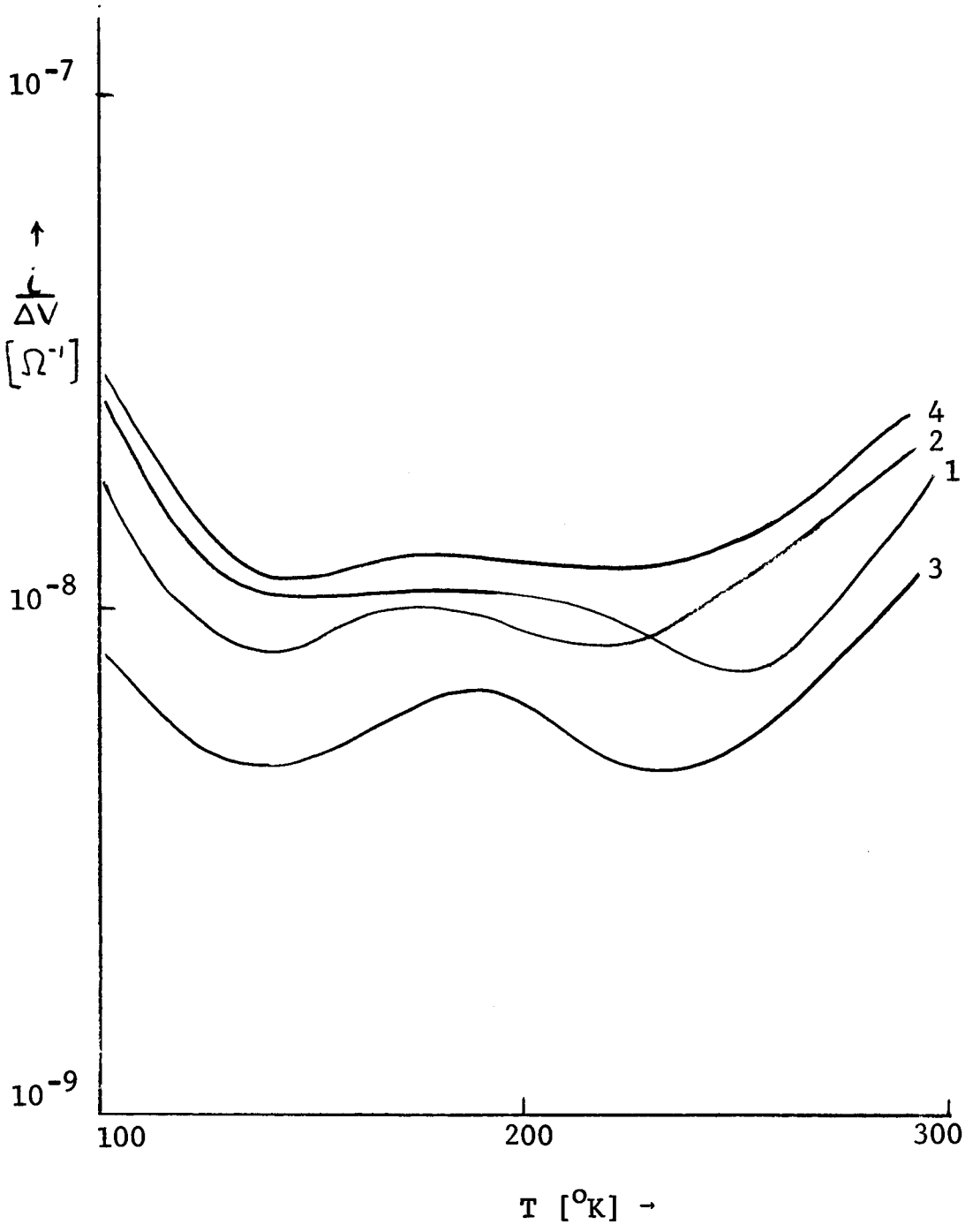

Figure 21. TSC curves for cadmium treated (closed tube) crystal 1) before and 2) after 300 keV irradiation at room temperature, 3) 6 days after and 4) after annealing at 100°C (490 mμ excitation).

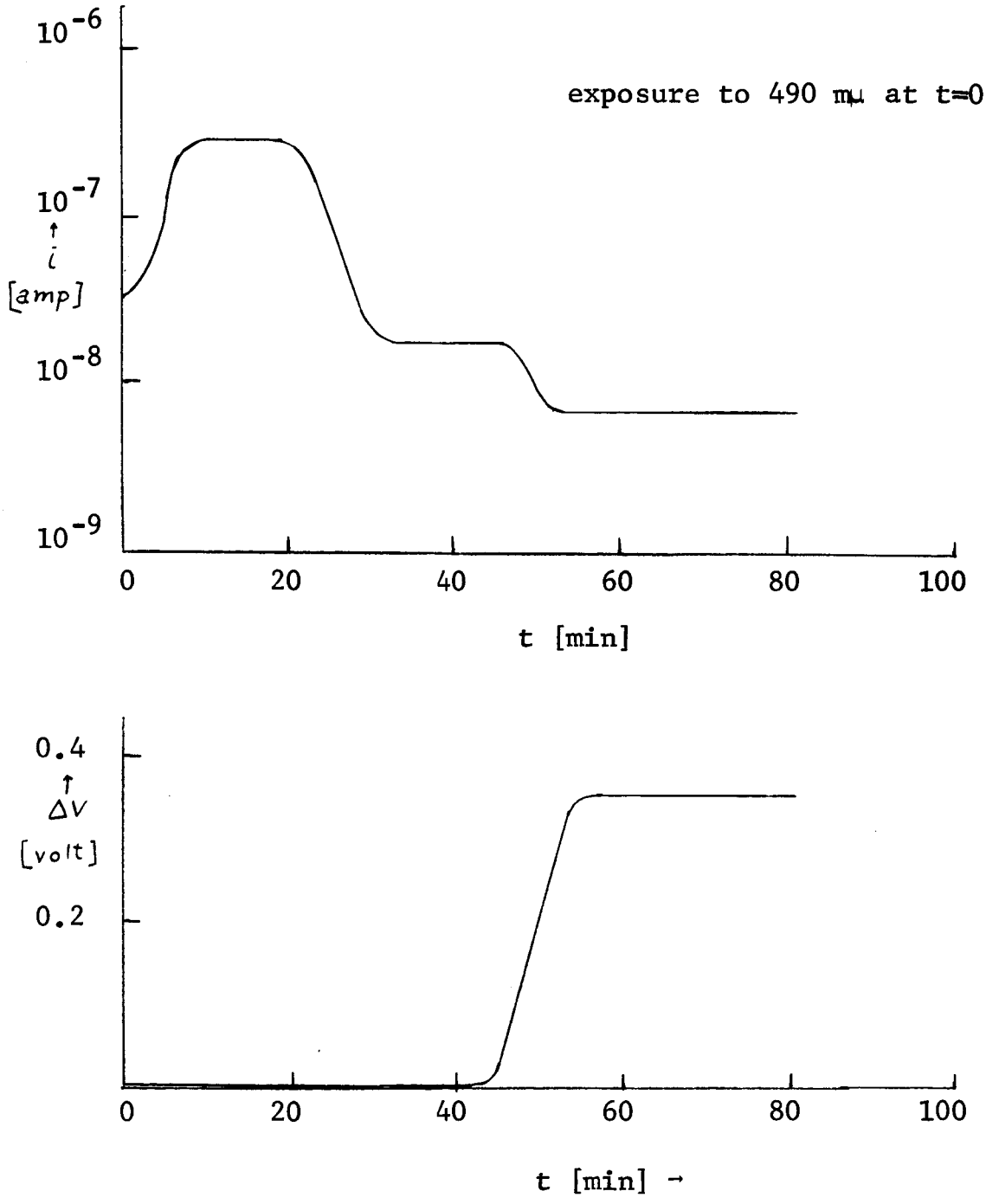

Figure 22. Current and probe voltage for cadmium treated (open tube) crystal after 300 keV x-ray irradiation at room temperature. Measured at -190°C.

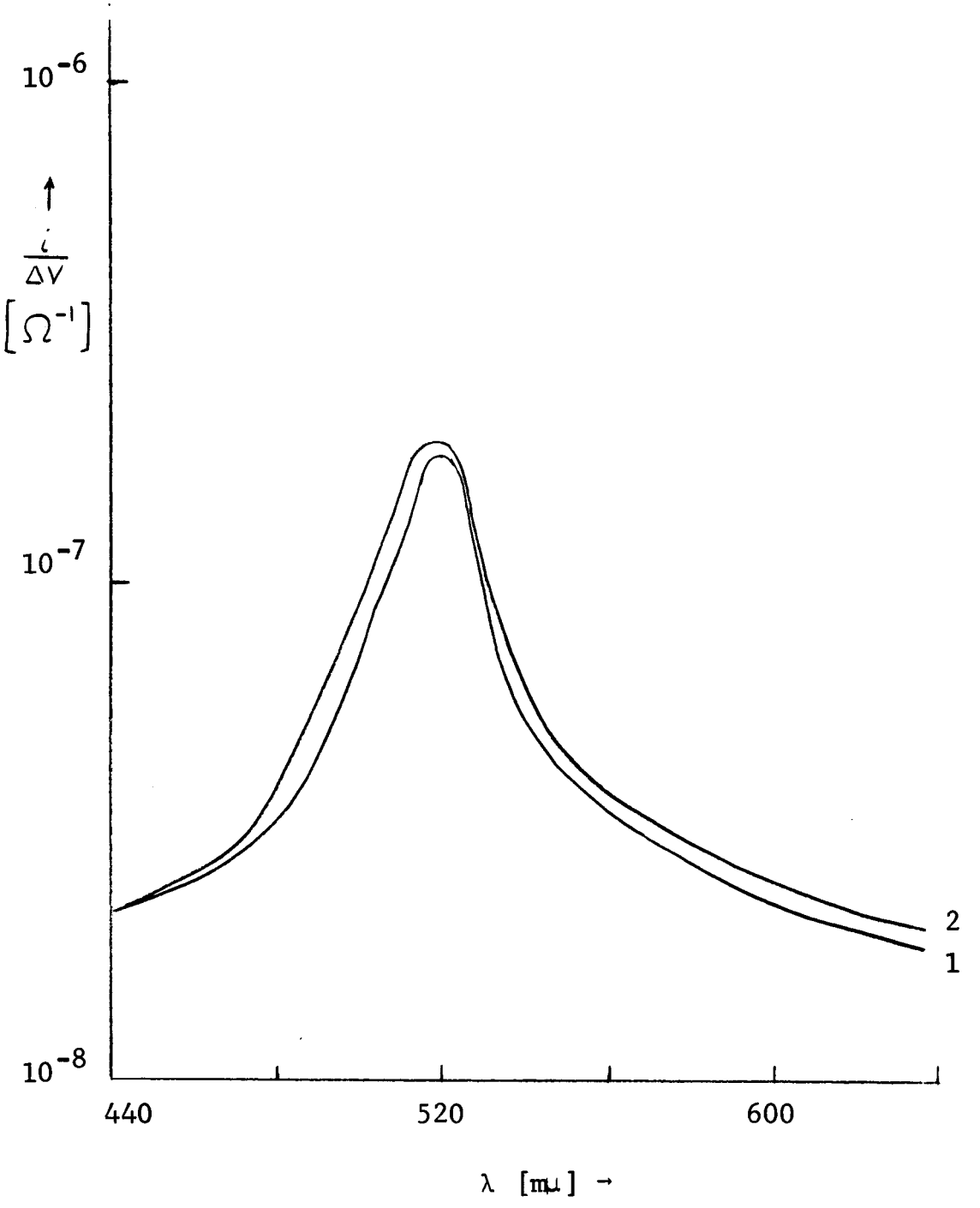

Figure 23. SDP for cadmium treated crystal (open tube) 1) before and 2) after 300 keV x-ray irradiation at room temperature. SDP measured at 25°C.

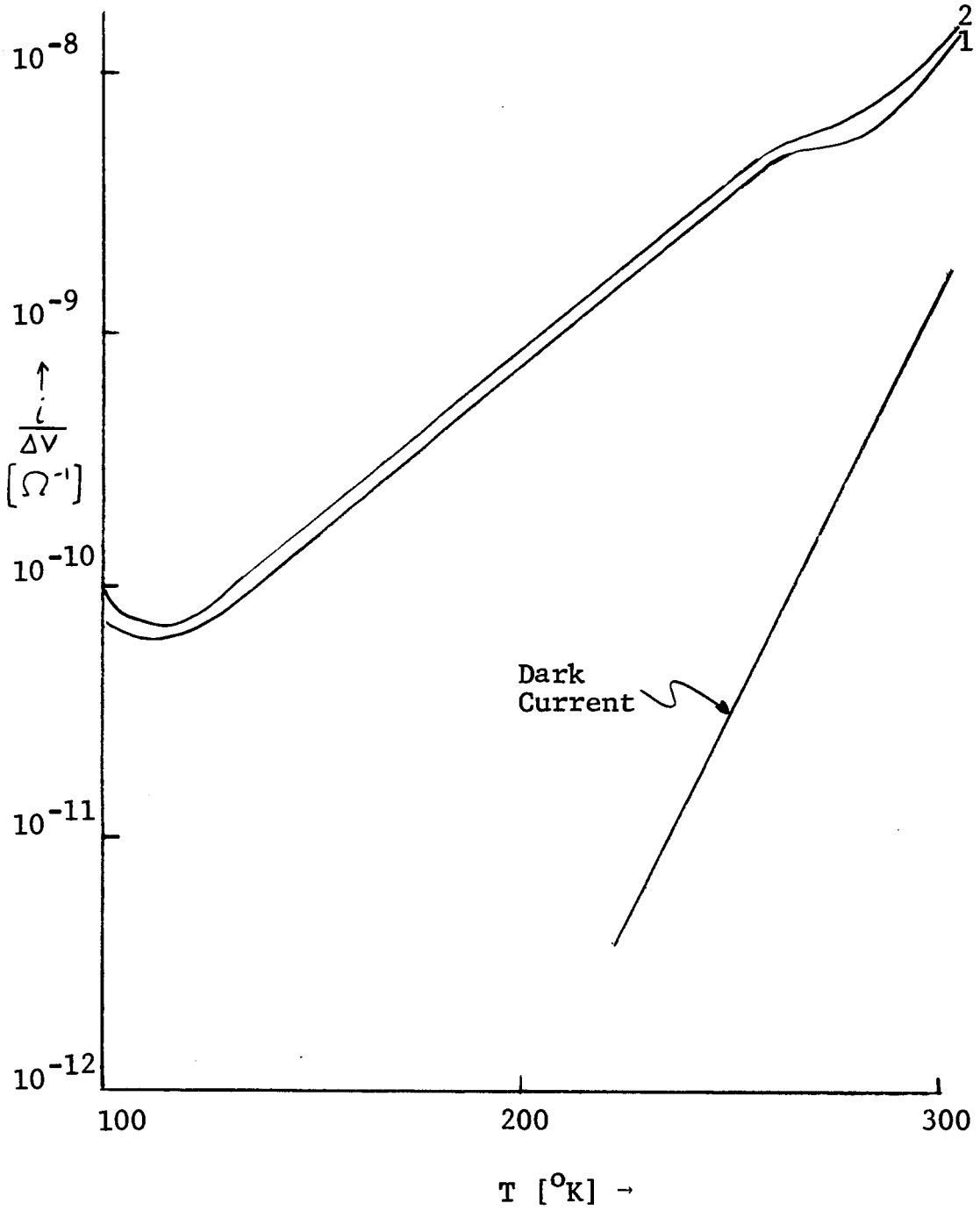

Figure 24. TSC curves for cadmium treated (open tube) crystal 1) before and 2) after 300 keV x-ray irradiation at 25°C.

CHAPTER V

Discussion of Results

The task now is to explain the experimental results in terms of specific defects. In doing so it must be remembered that the model proposed below in not a unique model for the explanation of the experimental results. The proposed model is however the most economical and employs the most probable defects produced in the lattice.

On the basis of section 2.2, the first energy threshold should be associated with damage in the sulfur sublattice, so it is proposed that the defects which occur for 300 keV irradiation are connected with the displacement of a sulfur atom from its lattice site. If we were to take 300 keV as the threshold energy, then the maximum energy transferred in a displacement collision is 27 eV. This amount of energy is about a factor of two greater than the displacement energy for germanium and silicon and even greater compared to values reported for compound semiconductors.

As can be seen from Appendix I, only 10^{12} photons in the energy range 250 to 300 keV are incident on the crystal during an irradiation while a change on the order of 10^{15} cm^{-3} is produced in the level at $E_c - E_t = 0.5$ eV. This indicates that photons of energy less than 250 keV must be important for the displacement process, however

since no level was detected in the photoconductivity measurements which corresponds to the 7200Å luminescence band of Kulp and Kelley[12] the 115 keV threshold proposed by them is not assumed here. An estimate using a quantum efficiency of one in Appendix I yields a value of 150 keV. A more precise value can be obtained by higher intensity or longer exposure time but neither was experimentally realizable with the x-ray source used.

The displacement of a sulfur atom occurs in an existing disordered region of the crystal where the sulfur, because of its large size, is more easily accomodated. Focusing collisions in particular enhance displacement at the crystal surfaces and produce isolated sulfur vacancies. This is in contrast to a recent calculation by Sanders[70] which predicts predominantly short range focusing collisions. In a previous calculation by Leibfreid[71], short and long range focusing collisions were equally weighted.

The decrease in the electron lifetime for room temperature irradiation, since it is wavelength independent, is attributed to the introduction of recombination centers into the crystal. Since there is no decrease for irradiation at -190°C, these centers do not form at this temperature but are produced when the crystal is warmed to room temperature. This fact indicates that the recombination centers are not the direct product of x-ray damage but involve a diffusion process. It is most probable that for formation of these recombination centers, some of the x-ray damage produced sulfur vacancies associate with one or more defects. The other defects may be intrinsic defects or impurities which form stable associates because of their charge character or

to minimize any lattice distortion. It is then necessary to state that sulfur vacancies become mobile at ~150°K since in Fig. 17, the TSC curve after irradiation begins to fall below the curve before irradiation at this point. This is comparable to vacancy diffusion at low temperature in other materials following irradiation. The diffusion of defects produced in a disordered region of the crystal may be stress enhanced and proceed for at least a few lattice constants, since appreciable self-diffusion occurs only at much higher temperatures.

If the recombination centers are active during the TSC measurements then after damaging the crystal, one would expect a shift to lower currents (Fig. 14, Curve 2'). Thus the actual curve (Curve 2) can be explained as a decrease in electron lifetime which leaves the 180°K peak unchanged while there is an increase in the density of defects responsible for the 300°K TSC peak. In agreement with work done by Bube and Barton[72] and Skarman[73] this peak is identified as caused by sulfur vacancies. Niekisch[66] also shows a slight increase in a level at 0.45 after 300 keV electron irradiation.

To recapitulate briefly, 300 keV x-rays are capable of producing sulfur displacement which occurs in some disordered region e.g. the crystal surface. The resultant sulfur vacancy produces a level at $E_c - E_t = 0.5$ eV while through a diffusion process some vacancies associate to form recombination centers. The fact that the sulfur vacancies are involved in the associates is further supported by the fact that after storing the crystals at room temperature there is a decrease in trap density as well as a decrease in the TSC peak current due to a change in electron lifetime (Fig. 14, Curve 3),

indicating a decrease in sulfur vacancies due to the formation of additional recombination centers.

The annealing of the damage occurs at a temperature between 100 and 150°C. This is the temperature at which enough thermal energy is available to break up the associates involving sulfur vacancies. The slight deviation from the pre-damaged state i.e. the shift of the SDP and TSC curves toward higher current can be explained by the effect of a vacuum heat treatment. Kennedy[40] has shown that in the temperature range of 50 to 350°C, vacuum heat treatment shifts the SDP to higher photocurrent because of the dissociation of associates acting as recombination centers. These centers dissociate to a large extent above 200°C indicating that they are different than the radiation damage produced centers, however wavelength independent increases by a factor of two were produced at 150°C and this effect is additive to the changes caused by the true annealing.

Consistent with the idea of defect creation at the surface of the crystal is the fact that succeeding irradiations produce less damage although the dose remains constant. Residual sulfur interstitials which remain in these regions due to incomplete annealing impedes the further formation of defects. In view of this fact, it should then be possible to saturate these regions by heat treatment in sulfur vapor. Although the changes in the defect structure are not completely understood for sulfur heat treatments of this type, it is certain that an excess of sulfur is provided at the surface during the cooling process after the treatment. Crystals treated in this manner when x-ray irradiated show that no defects are produced in detectable amounts. If the

crystals are then heat treated in vacuo at 350°C for one hour to produce partial evaporation of the excess sulfur from the surface, they revert to the damage-annealing cycles characteristic of the untreated crystals, although, as to be expected, the number of defects produced by x-rays is not as great.

Cadmium pre-treatment in a closed tube is unacceptable for the stoichiometry shifts sought here because the treatment must be carried out at low cadmium pressure for conservation of photosensitivity. In this case, a considerable contribution to the total pressure in the ampule is due to desorbed gas from the walls which may be responsible for changes at the surface e.g. formation of a CdO layer or doping by inward diffusion of impurities. These changes are reflected in the variation of dark conductivity of crystals treated in the same ampule and in persistent photoconductivity which is usually seen in doped crystals.

The SDP and TSC curves for the crystals heat treated in cadmium vapor in an open tube show that no damage is detected. The dark current versus temperature yield a slope of 0.4 eV which is characteristic of all investigated crystals treated in this way. Whether this corresponds to the Fermi level at this energy has not been fully investigated. However the shape of the TSC curve and the fact that the response times for these crystals are appreciably longer than for untreated crystals indicate a high density of traps above the Fermi level. These are masking the radiation damage defects. Production of comparable numbers of these defects is prevented by the intensity and exposure time of the x-ray source used.

The high conductivity state after x-ray irradiation is due to a sensitization of the crystal as discussed in Section 2.8. Similar high conductivity states have been seen after electron irradiation at 25 keV and above by Schulze and Kulp[74]. A more detailed discussion of the actual defects and the transitions involved in the sensitization and desensitization processes can not be given at this time.

In conclusion, the investigation reported here provides identification of the electron trap at $E_c-E_t=0.5$ eV as due to a sulfur vacancy. A recombination center is also detected which is an associate, one of whose members is also a sulfur vacancy. These levels may be produced by x-ray irradiation above a threshold which is estimated to be 150 keV. The defects produced can be annealed to a large extent by a vacuum heat treatment at $150^{o}C$. Displacement in the cadmium sublattice was not detected and a higher intensity of x-rays in the energy range extending from the displacement energy for sulfur is necessary for this investigation.

BIBLIOGRAPHY

1. R. H. Bube, J. Phys. Chem. Solids, 1, 234 (1957).
2. F. A. Kroger, H. J. Vink and Volger, Phil. Res. Rep., 10, 39 (1955).
3. R. H. Bube and S. M. Thomsen, J. Chem. Phys., 23, 15 (1955).
4. G. D. Watkins, J. W. Corbett and R. M. Walker, J. Appl. Phys., 30, 1198 (1959).
5. K. W. Böer, R. Boyn and O. Goede, Phys. Stat. Soc., 3, 1684 (1963).
6. R. Boyn, O. Goede and S. Kuschnerus, Phys. Stat. Sol., 12, 57, (1965).
7. F. Seitz and J. S. Kohler, Solid State Physics Vol. 2, Ed. F. Seitz and D. Turnbull, Academic Press Inc. New York (1956).
8. J. J. Loferski and P. Rappaport, Phys. Rev., 111, 432 (1958); J. Appl. Phys., 30, 1296 (1959).
9. W. L. Brown and W. M. Augustyniak, J. Appl. Phys., 30, 1300 (1959).
10. R. Bauerlein, Z. Naturforsch., 14a 1069 (1959).
11. F. H. Eiser and P. W. Bickel, Phys. Rev., 115, 345 (1959).
12. B. A. Kulp and R. H. Kelley, J. Appl. Phys., 31, 1057 (1960).
13. B. A. Kulp, Phys. Rev., 125, 1865 (1962).
14. B. A. Kulp and R. M. Detweiler, Phys. Rev. 129, 2422 (1963).
15. R. M. Detweiler and B. A. Kulp, Phys. Rev. 146, 513 (1966).
16. F. Seitz, Rev. Mod. Phys., 26, 7 (1954).
17. J. H. O. Varley, Nature 174, 886 (1954).
18. F. E. Williams, Phys. Rev. 126, 70 (1962).
19. G. F. J. Garlick, F. J. Bryant and A. F. J. Cox, Proc. Phys. Soc. 83, 967 (1964).

20. J. J. Loferski and P. Rappaport, J. Appl. Phys. 30, 1296 (1959).

21. W. L. Brown and W. M. Augustyniak, J. Appl. Phys. 30, 1300 (1959).

22. W. Kohn, Phys. Rev. 94, 1409 (1954).

23. M. W. Thompson, The Interaction of Radiation with Solids, Ed. R. Strumane et al. John Wiley and Sons Inc. New York (1964).

24. G. D. Watkins, 7th Internat Conf. on the Phys. of Semicond., Dunod, Paris (1965).

25. W. Van Gool and G. Diemer, Luminescence of Organic and Inorganic Material, Ed. H. P. Kallman and G. M. Spruch, John Wiley and Sons, Inc. New York.

26. K. Colbow, Phys. Rev. 141, 742 (1966).

27. F. A. Kroger, The Chemistry of Imperfect Crystals, John Wiley and Sons, Inc., New York, 1964.

28. W. Vieth, Z. Angew. Physik, 7, (1955).

29. D. Dutton, Phys. Rev. 112, 785 (1958).

30. R. H. Bube, Photoconductivity of Solids, John Wiley and Sons, Inc., New York, pp. 390-401 (1960).

31. R. H. Bube, J. Chem. Phys. 27, 4961 (1957).

32. P. Mark, Phys. Rev. 144, 751 (1966).

33. K. W. Böer and R. Schubert, Phys. Stat Sol. 16, K5 (1966).

34. J. T. Randall and M. H. F. Wilkins, Proc. Roy. Soc., 184, 365 (1945).

35. A. Bohun, Czech. J. Phys., 4, 91 (1954).

36. A. H. Booth, Canad. J. Chem., 32, 214 (1956).

37. W. Hoogenstraaten, Philips Res. Rep. 13, 515 (1958).

38. R. H. Bube, J. Chem. Phys. 23, 18 (1955).

39. I. A. Karpovich and B. N. Zvonkov, Soviet Phys.-Sol. State 6, 2714 (1965), FTT 6, 3392 (1964).

40. C. A. Kennedy, Masters Thesis, Univ. of Delaware, 1966.

41. W. T. Sproull, X-rays in Practice, McGraw-Hill Book Co., Inc., N.Y. 1946.

42. K. W. Böer, H. Berger and E. H. Weber Z. Phyisk 158, 501 (1960).

43. R. Hofstadter, Nucleonics 4, 2 (1949).

44. A. P. Galushka and I. D. Konozenko, Atom. Energ. 13, 277 (1962).

45. R. B. Oswald and C. Kikuchi, Tech. Rep. of College of Eng., Univ. of Michigan (1964).

46. K. W. Böer, E. H. Weber and B. Wojtowicz, Z. Physik 168, 115 (1962).

47. K. W. Böer and H. Gutjahr, Z. Physik 152, 203 (1958).

48. K. W. Böer, H. Berger and E. H. Weber, Z. Physik, 158, 501 (1960).

49. W. M. Butler and W. Muscheid, Ann. Phys. 15, 82 (1954).

50. J. Fassbender, Z. Physik 145, 301 (1956).

51. A. D. Galushka, I. B. Ermolovich, N.E. Korsunskaya, I. D. Konozenko and M. K. Sheinkman, Fiz. Tver. Tela 8, 1040 (66), Soviet Phys.-Sol. State 8, 831 (1966).

52. W. Schweinberger and D. Wruck, Phys. Stat. Sol. 15, 355 (1966).

53. R. Schubert, personal communication.

54. B. A. Kulp and R. H. Kelley, J. Appl. Phys. 32, 1290 (1961).

55. H. H. Woodbury, Phys. Rev. 134, A492 (1964).

56. E. A. Niekisch, Ann. Phys. 15, 279 (1955).

57. S. Tanaka and T. Tanaka, J. Phys. Soc. Japan 14, 113 (1959).

58. M. Barjon, C. Brachet, M. Lambert, M. Martineau and J. Schmouker, C. R. Acad. Sci. 248, 83 (1959).

59. V. I. Broser and R. Warminsky, Z. Naturforsch. 6a, 85 (1951).

60. T. Y. Sera, V. V. Serdyuk and I. M. Shevchenko, Fiz. Tver. Tela 3, 3537 (1961).

61. R. O. Chester, ORNL Report 3767, (1965).

62. S. Ibuki, J. Phys. Soc. Japan, 19, 1196 (1959).

63. V. D. Egorov, G. O. Müller and H. Weber, Phys. Stat. Sol. 12, 71 (1965).

64. M. R. Lorenz, M. Aven and H. H. Woodbury, Phys. Rev. 132, 143 (1963).

65. H. Saito, M. Kitagawa and M. Hirata, Proc. Japan Conf. on Radioisotopes 5, 207 (1963).

66. E. A. Niekisch, Semicond. Phys. Conf., Prague p. 1064 (1960).

67. R. J. Collins, J. Appl. Phys. 30, 1135 (1959).

68. W. Nalesnik, Personal communication.

69. R. Schubert, Personal communication.

70. J. B. Sanders, Physica 32, 2197 (1966).

71. G. Liebfried, J. Appl. Phys. 30, 1388 (1959).

72. R. H. Bube and L. A. Barton, RCA Review 20, 564 (1959).

73. J. S. Skarman, Solid State Electronics 8, 17 (1965).

74. R. G. Schulze and B. A. Kulp, J. Appl. Phys. 33, 2173 (1962).

75. E. A. Niekisch, Z. Phys. Chem. 216, 110 (1961).

76. W. Borchardt, Phys. Stat. Sol. 2, 1575 (1962).

77. K. W. Böer, W. Borchardt and S. Oberlander, Z. Phys. Chem. 210, 218 (1959).

APPENDIX I

A estimate of the number of photons incident on the crystal may be made using equation (10),

$$I_\lambda = C \frac{1}{\lambda^2} \left(\frac{1}{\lambda_o} - \frac{1}{\lambda} \right)$$

where $C = 3.13 \times 10^{-10}$ erg cm/s. I_λ gives the intensity as a function of wavelength λ and $I_\lambda \, d\lambda$ gives the energy radiated by the target in the range λ to $\lambda + d\lambda$. The total number of photons in this range is

$$n = \frac{I_\lambda \, d\lambda}{hc/\lambda}$$

$$= \frac{C}{hc} \frac{1}{\lambda} \left(\frac{1}{\lambda_o} - \frac{1}{\lambda} \right)$$

where h is Planck's constant and c is the speed of light. Therefore the number of photons per second radiated by the target in the energy range between the shortest wavelength λ_o and λ_1 may be found by integrating

$$N = \int_{\lambda_o}^{\lambda_1} \frac{C}{hc} \frac{1}{\lambda} \left[\frac{1}{\lambda_o} - \frac{1}{\lambda} \right] d\lambda$$

$$= \frac{C}{hc} \left[\frac{1}{\lambda_o} \ln {}^{\lambda_1}/_{\lambda_o} + \frac{1}{\lambda_1} - \frac{1}{\lambda_o} \right]$$

Assuming this is the total number of photons per second radiated into a solid angle of 2π, the total number of photons incident on the crystal is obtained by multiplying by a geometrical factor (1.2×10^{-4}) which takes into account the surface area of the crystal and by the exposure time (3.6×10^{3} s.). For $\lambda_o = 0.41\text{Å}$ to $\lambda_1 = 0.49\text{Å}$ which is the energy range 250 to 300 keV, $\sim 10^{12}$ photons are incident on the crystal.

There are $\sim 10^{15}$ cm^{-3} traps produced during an irradiation, so that if we assume a quantium efficiency of one (every photon absorbed above the threshold energy produces a displacement) a rough estimate of the threshhold energy can be determined by computing the λ_1 which will provide $\sim 10^{15}$ absorbed photons. The mass absorption constant in this region may be conveniently taken as 0.2 cm^2/gm. For this value, 6×10^{16} photons must be incident on the crystal to produce the desired number of defects. Using this number as N_{tot} in equation (10) $\lambda_1 = 8.6$ Å or the corresponding energy may be taken approximately as 150 keV.

APPENDIX II

Photochemical Reactions

Photochemical reactions, or the formation of defects through the influence of incident light have been reported in CdS by a number of investigators[75-77]. In one untreated crystal investigated, the following behavior was found: Initially the SDP curves made at room temperature were reproducible when measured on successive days. However after a damage-annealing cycle was carried out for an irradiation at 300 KeV at 25°C, the SDP was shifted to lower photocurrents for each successive measurement. The crystal remained in the dark at room temperature between measurements. Upon heating the crystal above 100°C, the measured SDP reproduced the original measurement (Fig. 25).

The crystal was also exposed to green light obtained by passing light from a Unitron source through a Corning CS-4-105 band pass filter. The photocurrent was monitored as a function of time and after a rise to a maximum value, the photocurrent decreased with time of exposure(Fig. 26). The effect of the light on the dark current was not obtained since the dark current was below the detection limit of the ammeter.

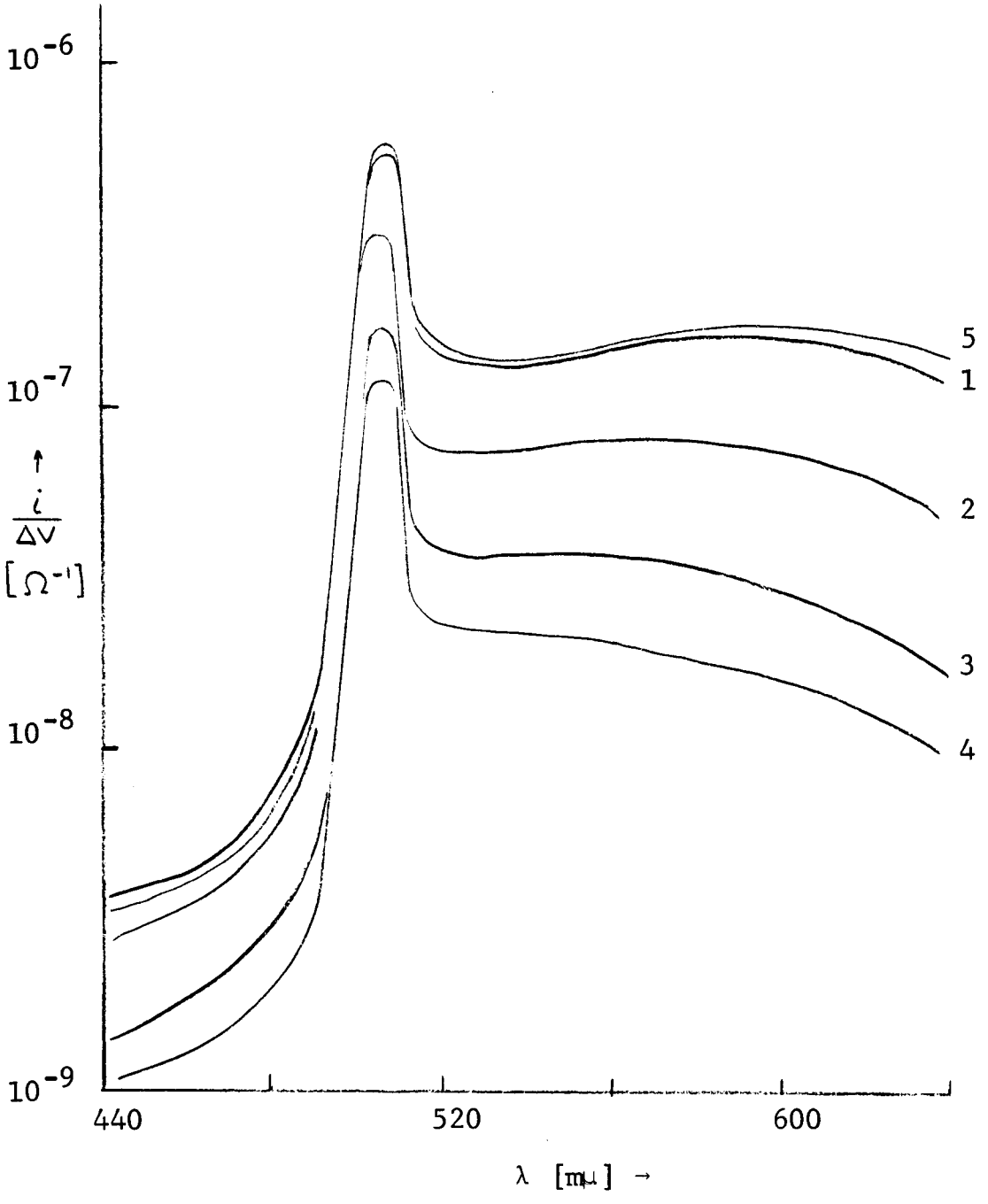

Figure 25. SDP curves 1) initial, 2) after 2 days, 3) after 6 days, 4) after 11 day and 5) after heating crystal to 100°C for one hour. SDP measured at 25°C.

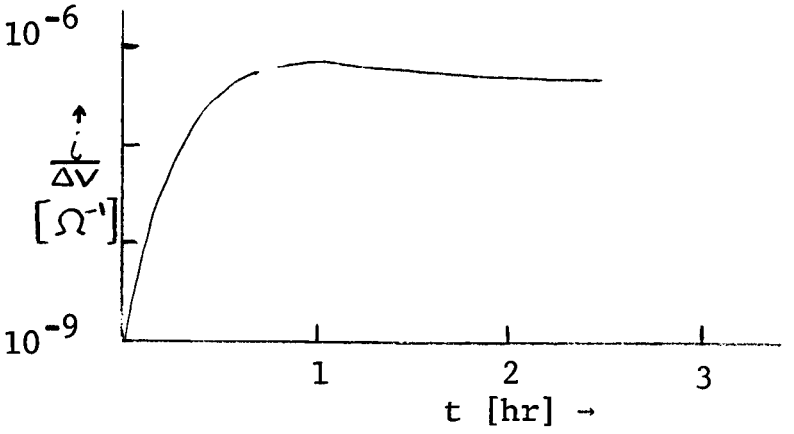

Figure 26

The wavelength independent decrease in electron lifetime is again most easily explained by the production of recombination centers. Niekisch[75] has proposed the formation of an associate of a sulfur vacancy and a cadmium vacancy which can occur above -35°C to account for a behavior of this type. This process could be favored because of coulomb attraction of the centers and the associates could be destroyed by a heat-treatment. While x-ray damage enhances production of photo chemical reactions, time considerations prevented a more thorough investigation. Since the SDP is quite reproducible for the crystals at -190°C, damage annealing cycles were performed with care taken not to expose the crystal to light at higher temperature.